unpublished data, 2011) or overexpression of these proteins[14] can decrease or increase, respectively, the stability of the DCV and, in turn, their half-life. Changes in the number of DCV transmembrane proteins can readily affect the stability of these vesicles. SNX19, however, is not a transmembrane protein, but, as determined by the yeast two hybrid system, binds to the cytoplasmic region of IA-2 encompassing amino acids 744–979[5]. Furthermore, SNX19 alone or the IA-2/SNX19 complex binds to several phosphatidylinositols (ptdlins), most strongly to Ptdins(3)P, Ptdlins(4)P and Ptdlins(5)P[16]. In contrast, IA-2 does not bind to the ptdlins. Ptdins(3)P is involved in the recruitment of many different proteins that are important for protein trafficking to membrane[17–19]. PtdIns(4)P is located in the membrane of the Golgi apparatus, and binds to the ADP ribosylation factor (ARF) GTP-binding protein and to four-phosphate-adaptor protein 1 and 2 (FAPP1 and FAPP2) and effector proteins[18,20]. This complex of molecules recruits proteins to the membrane. The function of PtdIns(5)P remains unknown, but it might act in membrane trafficking from late endosomes to the plasma membrane[20,21]. We suggest that binding of the IA-2/SNX19 complex to the ptdlins might be responsible for sorting, trafficking and stabilization of the DVC. In SNX19KD MIN6 cells, lysosomal activities are increased, restored by reintroduction of SNX19 or IA-2. Knockdown of SNX19 decreases IA-2 expression; reintroduction of SNX19 increases IA-2 expression in MIN6 cells. Thus, SNX19 regulates IA-2 expression to allow a complex of SXN19 and IA-2 to stabilize the DCV. Decreased expression of SNX19 reduces IA-2 expression and destabilizes DCV, resulting in increasing lysosomal activities and decreasing DCV half-life. Although the mechanism is not known precisely, based on our findings, the binding of SNX19 to IA-2 might be directly involved in the stabilization of DCV by exposing or protecting IA-2 from degradation or by affecting trafficking or recycling of the DCV through the endosome pathway.

SNX19 also was found to affect cell proliferation. Knockdown of SNX19 inhibited cell proliferation, which was restored by reintroduction of SNX19. We previously reported that overexpression of IA-2 and/or SNX19 induced apoptosis and inhibited cell proliferation together with a decrease in Akt/PKB phosphorylation under high glucose conditions[16]. In contrast, knockdown of IA-2 and/or SNX19 did not induce apoptosis in β-cells (data not shown). However, cell proliferation was inhibited in SNX19 knockdown MIN6 cells with a decrease in insulin content and insulin secretion. On the other hand, reintroduction of SNX19 or IA-2 restored cell proliferation in SNX19KD MIN6 cells with an increase in insulin content and insulin secretion. A possible explanation is that a decrease in insulin secretion, which is important for cell growth in pancreatic β-cells, contributes to inhibition of cell proliferation in SNX19KD MIN6 cells.

In conclusion, the present study shows the importance of SNX19 in DCV physiology. Recent studies have shown that SNX19 can bind not only to IA-2, but also to IA-2β (S.-I. Harashima, unpublished data, 2011). As there are nearly 30 different members of the SNX family, it is an intriguing group of proteins for further study.

ACKNOWLEDGEMENTS

This study was supported by Scientific Research Grants from the Ministry of Education, Culture, Sports, Science, and Technology, Japan, and from the Ministry of Health, Labor, and Welfare, Japan, and also by Kyoto University Global COE Program 'Center for Frontier Medicine'.

REFERENCES

1. Worby CA, Dixon JE. Sorting out the cellular functions of sorting nexins. *Nat Rev Mol Cell Biol* 2002; 3: 919–931.
2. Cullen PJ. Endosomal sorting and signaling: an emerging role for sorting nexins. *Nat Rev Mol Cell Biol* 2009; 9: 574–582.
3. Xu Y, Seet LF, Hanson B, *et al.* The phox homology (PX) domain, a new player in phosphoinositide signaling. *Biochem J* 2001; 360: 513–530.
4. Seet LF, Hong W. The Phox (PX) domain proteins and membrane traffic. *Biochim Biophys Acta* 2006; 1761: 878–896.
5. Hu YF, Zhang HL, Cai T, *et al.* The IA-2 interactome. *Diabetologia* 2005; 48: 2576–2581.
6. Lan MS, Lu J, Goto Y, *et al.* Molecular cloning and identification of a receptor-type protein tyrosine phosphatase, IA-2, from human insulinoma. *DNA Cell Biol* 1994; 13: 505–514.
7. Notkins AL, Lernmark A. Autoimmune type 1 diabetes: resolved and unresolved issues. *J Clin Invest* 2001; 108: 1247–1252.
8. Magistrelli G, Toma S, Isacchi A. Substitution of two variant residues in the protein tyrosine phosphatase-like PTP35/IA-2 sequence reconstitutes catalytic activity. *Biochem Biophys Res Commun* 1996; 227: 581–588.
9. Saeki K, Zhu M, Kubosaki A, *et al.* Target disruption of the protein tyrosine phosphase-like molecule IA-2 results in alterations in glucose tolerance tests and insulin secretion. *Diabetes* 2002; 51: 1284–1850.
10. Kubosaki A, Nakamura S, Notkins AL. Dense core vesicle protein IA-2 and IA-2{beta}: metabolic alterations in double knockout mice. *Diabetes* 2005; 54: s46–s51.
11. Kubosaki A, Nakamura S, Clark A, *et al.* Disruption of the transmembrane dense core vesicle proteins IA-2 and IA-2β causes female infertility. *Endocrinology* 2006; 147: 431–438.
12. Nishimura T, Kubosaki A, Ito Y, *et al.* Disturbances in the secretion of neurotransmitters in IA-2/IA-2beta null mice: changes in behavior, learning and lifespan. *Neuroscience* 2009; 159: 427–437.
13. Kim SM, Power A, Brown TM, *et al.* Deletion of the secretory vesicle proteins IA-2 and IA-2beta disrupts circadian rhythms of cardiovascular and physical activity. *FASEB J* 2009; 23: 3226–3232.

14. Harashima S, Clark A, Christie MR, *et al.* The dense core transmembrane vesicle protein IA-2 is a regulator of vesicle number and insulin secretin. *Proc Natl Acad Sci USA* 2005; 102: 8704–8709.
15. Nishimura T, Harashima S, Hu YF, *et al.* IA-2 modulates dopamine secretion in PC12 cells. *Mol Cell Endocrinol* 2010; 315: 81–86.
16. Harashima SI, Harashima C, Nishimura T, *et al.* Overexpression of the autoantigen IA-2 puts beta cells into a pre-apoptotic state: autoantigen-induced, but non-autoimmune-mediated, tissue destruction. *Clin Exp Immunol* 2007; 15: 49–60.
17. Lemmon MA. Phosphoinositide recognition domains. *Traffic* 2003; 4: 201–213.
18. Roth MG. Phosphoinositides in constitutive membrane traffic. *Physiol Rev* 2004; 84: 699–730.
19. Kutateladze TG. Mechanistic similarities in docking of the FYVE and PX domains to phosphatidylinositol 3-phosphate containing membrane. *Prog Lipid Res* 2007; 46: 315–327.
20. Sasaki T, Sasaki J, Sakai T, *et al.* The physiology of phosphoinositides. *Bio Pharm Bull* 2007; 30: 1599–1604.
21. Ooms LM, Horan KA, Rahman P, *et al.* The role of the inositol polyphosphate 5-phosphatases in cellular function and human disease. *Biochem J* 2009; 419: 29–49.

THE JOURNAL OF BIOLOGICAL CHEMISTRY VOL. 288, NO. 3, pp. 1929–1938, January 18, 2013

Transcriptional Regulatory Factor X6 (Rfx6) Increases Gastric Inhibitory Polypeptide (GIP) Expression in Enteroendocrine K-cells and Is Involved in GIP Hypersecretion in High Fat Diet-induced Obesity*

Received for publication, September 27, 2012, and in revised form, November 28, 2012 Published, JBC Papers in Press, November 28, 2012, DOI 10.1074/jbc.M112.423137

Kazuyo Suzuki, Norio Harada, Shunsuke Yamane, Yasuhiko Nakamura, Kazuki Sasaki, Daniela Nasteska, Erina Joo, Kimitaka Shibue, Takanari Harada, Akihiro Hamasaki, Kentaro Toyoda, Kazuaki Nagashima, and Nobuya Inagaki[1]

From the Department of Diabetes and Clinical Nutrition, Graduate School of Medicine, Kyoto University, 54 Kawahara-cho, Shogoin, Sakyo-ku, Kyoto 606-8507, Japan

Background: Gastric inhibitory polypeptide (GIP) secreted from enteroendocrine K-cells potentiates insulin secretion and induces energy accumulation into adipose tissue.
Results: Transcriptional Rfx6 is expressed in K-cells and increases GIP expression. Rfx6 expression is up-regulated in K-cells of obese mice.
Conclusion: Rfx6 plays critical roles in GIP expression and hypersecretion in obesity.
Significance: Gene analysis of K-cells isolated from GIP-GFP knock-in mice enabled identification of Rfx6.

Gastric inhibitory polypeptide (GIP) is an incretin released from enteroendocrine K-cells in response to nutrient ingestion. GIP potentiates glucose-stimulated insulin secretion and induces energy accumulation into adipose tissue, resulting in obesity. Plasma GIP levels are reported to be increased in the obese state. However, the molecular mechanisms of GIP secretion and high fat diet (HFD)-induced GIP hypersecretion remain unclear, primarily due to difficulties in separating K-cells from other intestinal epithelial cells *in vivo*. In this study, GIP-GFP knock-in mice that enable us to visualize K-cells by enhanced GFP were established. Microarray analysis of isolated K-cells from these mice revealed that transcriptional regulatory factor X6 (Rfx6) is expressed exclusively in K-cells. *In vitro* experiments using the mouse intestinal cell line STC-1 showed that knockdown of Rfx6 decreased mRNA expression, cellular content, and secretion of GIP. Rfx6 bound to the region in the *gip* promoter that regulates *gip* promoter activity, and overexpression of Rfx6 increased GIP mRNA expression. HFD induced obesity and GIP hypersecretion in GIP-GFP heterozygous mice *in vivo*. Immunohistochemical and flow cytometry analysis showed no significant difference in K-cell number between control fat diet-fed (CFD) and HFD-fed mice. However, GIP content in the upper small intestine and GIP mRNA expression in K-cells were significantly increased in HFD-fed mice compared with those in CFD-fed mice. Furthermore, expression levels of Rfx6 mRNA were increased in K-cells of HFD-fed mice. These results suggest that Rfx6 increases GIP expression and content in K-cells and is involved in GIP hypersecretion in HFD-induced obesity.

Obesity leads to insulin resistance characterized by fasting hyperinsulinemia and excessive insulin secretion to maintain euglycemia after meal ingestion (1). Obesity is an important risk factor in progression to type 2 diabetes mellitus (2) as well as cardiovascular disease (3), and reduction of obesity can normalize hyperinsulinemia and impede the progression of diabetes and arteriosclerosis.

Gastric inhibitory polypeptide, also called glucose-dependent insulinotropic polypeptide (GIP),[2] and glucagon-like peptide-1 (GLP-1) are the incretins, peptide hormones released from the gastrointestinal tract into circulation in response to meal ingestion that potentiate glucose-stimulated insulin secretion (4, 5). GIP is secreted from enteroendocrine K-cells located in the duodenum and upper small intestine; GLP-1 is secreted from enteroendocrine L-cells located in the lower small intestine and colon. GIP binds to the GIP receptor (GIPR) on the surface of pancreatic β-cells, adipose tissue, and osteoblasts, and it stimulates insulin secretion (6), fat accumulation (7), and bone formation (8), respectively, by increasing the level of intracellular adenosine 3′,5′-monophosphate (cAMP).

It was reported previously that GIPR-deficient mice exhibit insufficient compensatory insulin secretion upon high fat loading (9), suggesting that GIP plays a critical role in maintaining blood glucose levels by hypersecretion of insulin in diet-induced obesity. We also reported that sensitivity of GIPR to GIP in β-cells is increased in high fat diet (HFD)-induced obese mice (10). In addition, GIPR is expressed in adipose tissue (11) and increases glucose and triglyceride uptake in fat cells (12, 13). Thus, GIP has both direct and indirect effects on the accumulation of energy into adipose tissue. Some studies report that GIP secretion is increased in obesity (7, 14–16) and that pancreatic and duodenal homeobox 1 (Pdx1), which is known to be

* This work was supported by scientific research grants from the Ministry of Education, Culture, Sports, Science, and Technology, Japan, the Ministry of Health, Labor, and Welfare, Japan, and scientific research grants from the Japan Diabetes Foundation.
[1] To whom correspondence should be addressed. Tel.: 81-75-751-3562; Fax: 81-75-751-6601; E-mail: inagaki@metab.kuhp.kyoto-u.ac.jp.

[2] The abbreviations used are: GIP, gastric inhibitory polypeptide; GIPR, GIP receptor; HFD, high fat diet; CFD, control fat diet; EGFP, enhanced GFP; OGTT, oral glucose tolerance test.

an important transcription factor in pancreatic development and pancreatic β-cell maturation (17), has a critical role in GIP production in K-cells (18, 19). However, the mechanisms involved in GIP hypersecretion from K-cells in obesity remain unclear due to difficulties in separating these cells from other intestinal epithelial cells *in vivo*.

In this study, we investigated expression of various genes in K-cells by using GIP-GFP knock-in (GIP-GFP) mice in which K-cells can be visualized by EGFP fluorescence. We found that regulatory factor X6(Rfx6) is expressed exclusively in K-cells of the upper small intestine and is involved in GIP mRNA expression in the mouse small intestinal cell line STC-1. Furthermore, expression of Rfx6 as well as Pdx1 was found to be increased in K-cells of HFD-induced obese mice. Thus, GIP expression is stimulated by both Rfx6 and Pdx1, suggesting that these transcription factors play an important role in both GIP expression and GIP hypersecretion in HFD-induced obesity.

EXPERIMENTAL PROCEDURES

Animals—We designed targeting vector constructs as short-EGFP-poly(A)-loxp-Neo-loxp-long cassettes using mouse B6N BAC clone (identification numbers RP23-31E4 and RP23-383D10). A diphtheria toxin A expression cassette for negative selection was attached to the 3′ end of the *gip* sequence in the targeting vector. Next, the targeting vector was injected in embryonic stem cells from C57BL/6 mice, and a Neo resistance strain was established. The ES cells positive for the knock-in gene were selected by Southern blot analysis. The established ES cells were then injected into the blastocyst to obtain chimeric mice. Finally, we generated hetero-mutant mice by mating the chimeric mice with wild-type C57BL/6 mice. The mice were housed in an air-controlled (temperature 25 °C) room with a dark-light cycle of 10 and 14 h, respectively. Animal care and procedures were approved by the Animal Care Committee of Kyoto University.

GIP-GFP heterozygous mice (7 weeks of age) were fed control fat chow (CFD; 10% fat, 20% protein, and 70% carbohydrate by energy) or high fat chow (HFD; 60% fat, 20% protein, and 20% carbohydrate by energy) (Research Diets Inc., New Brunswick, NJ) for 8 weeks. Food intake, water intake, and body weight were measured.

Immunohistochemistry—Mouse upper small intestine samples were fixed in Bouin's solution and transferred into 70% ethanol before processing through paraffin. Rehydrated paraffin sections were incubated overnight at 4 °C with primary mouse anti-GFP antibody (sc-9996, 1:100, Santa Cruz Biotechnology) and rabbit anti-GIP antibody (T-4053, 1:100, Peninsula Laboratories, Inc., San Carlos, CA). Intestine samples and STC-1 cells (kindly provided by Prof. Hanahan, University of California, San Francisco) were embedded by Tissue-Tek O.C.T. compound 4583 (Sakura Fine Technical Co. Ltd., Tokyo, Japan) and immediately frozen in liquid nitrogen. Frozen sections (10 μm) on slides were air-dried and fixed in acetone for 5 min. Slides were then washed in phosphate-buffered saline (PBS) and blocked for 15 min in 3% BSA. They were incubated overnight at 4 °C with primary antibody (mouse anti-GIP antibody (1:100, kindly provided by Merck Millipore)) and goat anti-Rfx6 antibody (ABD28, 1:100, Merck). The sections were incubated for 1 h at room temperature with secondary antibody. Images were taken using a fluorescent microscopy with a BZ-8100 system (KEYENCE Corp., Osaka, Japan) and confocal microscopy with an LSM510META system (Carl Zeiss Co., Ltd., Jena, Germany).

Fifty representative mucous membranes from each slide were randomly selected, and their mean length and GFP-positive cells were quantified using fluorescent microscopy images. To count the GFP-positive cells, we distinguished the mucous membrane as villus, upper crypt, or lower crypt.

Isolation of K-cells from Mouse Intestinal Epithelium—Mouse upper small intestine was removed and washed by PBS. The intestine was cut into several round pieces and tied on one side with a thread. The pouch-like intestine was injected with Hanks' balanced salt solution containing 0.5 mg/ml collagenase, clamped, and incubated with CO_2 at 37 °C for 10 min in Krebs-Ringer bicarbonate buffer (KRBB: 120 mM NaCl, 4.7 mM KCl, 1.2 mM $MgSO_4$, 1.2 mM KH_2PO_4, 2.4 mM $CaCl_2$, 20 mM $NaHCO_3$). The digested intestinal epithelium was collected into the tube filled with Roswell Park Memorial Institute (RPMI) medium and rinsed twice. The intestinal epithelium was cultured in a humidified incubator (95% air and 5% CO_2) at 37 °C for 1 h. Afterward, it was centrifuged at 180 × *g* for 5 min, resuspended in PBS twice, and filtered with a cell strainer (352340, Falcon cell strainer, BD Biosciences). GFP-positive cells in the intestinal epithelium were analyzed using BD FACS Aria™ flow cytometer (BD Biosciences). Sorted cells were collected into vials containing medium at a rate of 2000 cells/tube.

Total RNA was extracted with PicoPure RNA isolation kit (Applied Biosystems, Inc., Alameda, CA) from sorted cells of GIP-GFP mouse intestinal epithelium and treated with DNase (Qiagen Inc., Valencia, CA). Microarray analysis was performed using GeneChip Mouse Genome 430 2.0 Array (Affymetrix Inc., Fremont, CA).

Glucose Tolerance Test (OGTT) and GIP Assay—After a 16-h fasting period, OGTTs (1 g/kg body weight) were performed. Blood samples were taken at the indicated times (0, 15, 30, 60, and 120 min after glucose loading), and blood glucose levels, plasma insulin levels, and plasma total GIP concentrations were measured. Blood glucose levels were determined by the glucose oxidase method (Sanwa Kagaku Kenkyusho Co. Ltd., Nagoya, Japan). Plasma insulin levels were determined using enzyme immunoassay (Shibayagi, Gumma, Japan). Plasma total GIP levels were determined using an ELISA kit (Merck Millipore).

For measurement of GIP content in the mouse upper small intestine, the mice were killed at 15 weeks of age after 8 weeks of CFD or HFD feeding. The intestine was rapidly removed and washed in PBS. After measuring the weight, samples were extracted with 5 ml/g acid ethanol, and GIP levels were measured (15).

Quantitative RT-PCR—Complementary DNA (cDNA) was prepared by reverse transcriptase (Invitrogen) with an oligo(dT) primer (Invitrogen). Messenger RNA (mRNA) levels were measured by quantitative RT-PCR using ABI PRISM 7000 Sequence Detection System (Applied Biosystems Inc.). PCR analyses were carried out using the oligonucleotide primers. SYBR Green PCR master mix (Applied Biosystems Inc.) was prepared for PCR run. Thermal cycling conditions were dena-

turation at 95 °C for 10 min followed by 50 cycles at 95 °C for 15 s and 60 °C for 1 min. C- and N-terminal primers of target molecules were designed as follows: GIP forward, 5′-gtggctttgaagacctgctc-3′, and reverse, 5′-ttgttgtcggatcttgtcca-3′; GFP forward, 5′-gtggctttgaagacctgctc-3′, and reverse, 5′-tttacgtcgccgtccagctcg-3′; GLP-1 forward, 5′-tgaagacaaacgccactcac-3′, and reverse, 5′-tcatgacgtttggcaatgtt-3′; Pdx1 forward, 5′-gacctttcccgaatggaa-3, and reverse, 5′-cttgttttcctcgggttc-3′; Rfx1 forward, 5′-gcagccagaagcagtatgtg-3′, and reverse, 5′-tggcttctgacacagtctcact-3′; Rfx2 forward, 5′-cagaactccgagggaggag-3′, and reverse, 5′-ggagggtgagtgtctgcatc-3′; Rfx3 forward, 5′-cgtcacaggaggacaactca-3′, and reverse, 5′-cagacttttgcagcgtctca-3′; Rfx4 forward, 5′-ccgaatacactggccttagc-3′, and reverse, 5′-atgggtgctcctcatacagg-3′; Rfx5 forward, 5′-tctaccttcagctccatcg-3′, and reverse, 5′-ggcaggtatccatgtgctct-3′; Rfx6 forward, 5′-acagacacggaatctgacat-3′, and reverse, 5′-ctctaccacagtgtccaacc-3′; Rfx7 forward, 5′-cgctctgcaacacaagatca-3′, and reverse, 5′-gaccagaaggcagttgaagg-3′; and GAPDH forward, 5′-aaatggtgaaggtcggtgtg-3′, and reverse, 5′-tcgttgatggcaacaatctc-3′.

Cell Culture and Small Interfering RNA (siRNA) Transfection into STC-1 Cells—STC-1 cells, mouse small intestinal cell line, were cultured in Dulbecco's modified Eagle's medium (DMEM) (Sigma) supplemented with 10% heat-inactivated fetal calf serum, 100 IU/ml penicillin, and 100 μg/ml streptomycin at 37 °C in a humidified atmosphere (5% CO_2 and 95% air). siRNA transfection of Stealth™ siRNAs were synthesized (Invitrogen). The sequences of siRNAs specific for Rfx6 and Pdx1 are shown as follows: Pdx1, caguacuacgcggccacacagcucu and agagcugugguggccgcguaguacug, and Rfx6, ggugaaugccaugguaucugauauu and aauaucagauaccauggcauucacc. Cultured STC-1 cells were trypsinized, suspended with DMEM without antibiotics, mixed with Opti-MEM (Invitrogen) containing siRNA and Lipofectamine TM2000 (Invitrogen), plated on 12-well dishes, and then incubated at 37 °C in a CO_2 incubator. The amounts of STC-1 cells were 1×10^6 cells/well. Medium was replaced with 1 ml of DMEM containing antibiotics about 5–6 h after transfection. RT-PCR was performed 48 h after transfection.

Plasmid Construction and Transfection into STC-1 Cells—The cDNA fragment of mouse Rfx6 protein was obtained from mouse (C57BL/6) islets by RT-PCR. The cDNA fragment of Rfx6 was cloned into pCMV vector (Clontech). Expression plasmids of Rfx6 cDNA were transfected into STC-1 cells using Lipofectamine™ 2000 (Invitrogen). Plasmid (8 μg/well) was diluted into Opti-MEM, and Lipofectamine™ 2000 was added and incubated at room temperature for 20 min. After incubation, the mixture was added to STC-1 cells (1×10^6 cells/well). RT-PCR was performed 48 h after transfection.

Measurement of Incretin Release and Cellular Content in STC-1 Cells—For incretin release assays, DMEM was collected from STC-1 cells cultured on 12-well dishes about 42–43 h after changing the medium (48 h after transfection). Media were centrifuged at 3000 × *g* for 10 min, and the supernatant was collected. Total GIP and total GLP-1 levels were measured by ELISA methods (Merck Millipore and Meso Scale Discovery (Gaithersburg, MD), respectively) as incretin release from STC-1 cells.

To determine incretin content, STC-1 cells cultured on 12-well dishes (48 h after transfection) were washed with PBS and homogenized in 0.5 ml of 0.1 N HCl and extracted at RT for 10 min, after which the supernatant was collected and centrifuged at 3000 × *g* for 10 min. Incretin and protein levels were measured by ELISA (GIP and GLP-1) and Bradford reagent (Bio-Rad), respectively.

Yeast One-hybrid Assay—Yeast one-hybrid assays were performed using the Matchmaker Gold Yeast One-hybrid Library Screening System (Clontech) according to the manufacturer's protocol. The *gip* promoter fragments shown in Fig. 4*A* were inserted separately upstream of the aureobasidin A resistance gene on the pAbAi vector, and Rfx6 cDNA was inserted downstream of GAL4-activating domain (GAL4AD) on the pGADT7 activating domain vector. The interactions between *gip* promoter fragments and Rfx6-GAL4AD protein were assayed using the aureobasidin A resistance gene reporter system. First, *Saccharomyces cerevisiae* Y1HGold (*MATα, ura3-52, his3-200, ade2-101, trp1-901, leu2-3, 112, gal4Δ, gal80Δ, met-MEL1*) was transformed by *gip* promoter fragment-inserted pAbAi plasmid (pAbAi-fragments a, b, c, and d), and spread on the synthetic medium with dextrose (SD) (without uracil) and incubated for 1 week at 30 °C. Obtained yeast was transformed by Rfx6 cDNA-inserted pGADT7 activating domain plasmid (pGADT7-Rfx6), spread on the SD (without tryptophan) medium, and then incubated for 1 week at 30 °C. Interaction between *gip* promoter fragment and Rfx6-GAL4AD protein could be detected, and the transformant was grown on SD (without tryptophan) medium containing 600 ng/ml aureobasidin A.

GIP Promoter Activity—1×10^6 STC-1 cells were cotransfected with pGL4.19 luciferase reporter plasmid expressing five different lengths of the *gip* promoter gene (Fig. 4*C*) and pGL4.73 *Renilla* luciferase reporter plasmid. 48 h after transfection, luciferase and *Renilla* activities were assayed according to the manufacturer's protocol (Promega Corp., Madison, WI) using a GioMax 20/20n luminometer (Promega). Firefly luciferase activity was normalized to *Renilla* luciferase expression and is presented as fold increase in relative light units over samples transfected with pGL4.19. All samples were analyzed in duplicate.

Analysis—The results are given as means ± S.E. (S.E., n = number of mice). Statistical significance was determined using paired and unpaired Student's t test and analysis of variance. $p \leq 0.05$ was considered significant.

RESULTS

Visualization and Isolation of K-cells Using GIP-GFP Mice—GIP-GFP mice were generated for the purpose of visualizing enteroendocrine K-cells (Fig. 1*A*). The mouse *gip* gene is composed of six exons. The targeting vector for GIP-GFP mice was designed so that EGFP cDNA was fused with exon 3 in the *gip* gene. Prepro-GIP consists of 144 amino acids (Fig. 1*B*), and PC1/3 and PC2 cleave prepro-GIP, generating GIP(1–42) and GIP(1–30), respectively. In GIP-GFP mice, the fusion protein retains the signal peptide, but it does not have the GIP(1–42) sequence nor the PC1/3 and PC2 cleavage sites. Accordingly, GIP-GFP mice express GIP signal peptide-GFP fusion protein

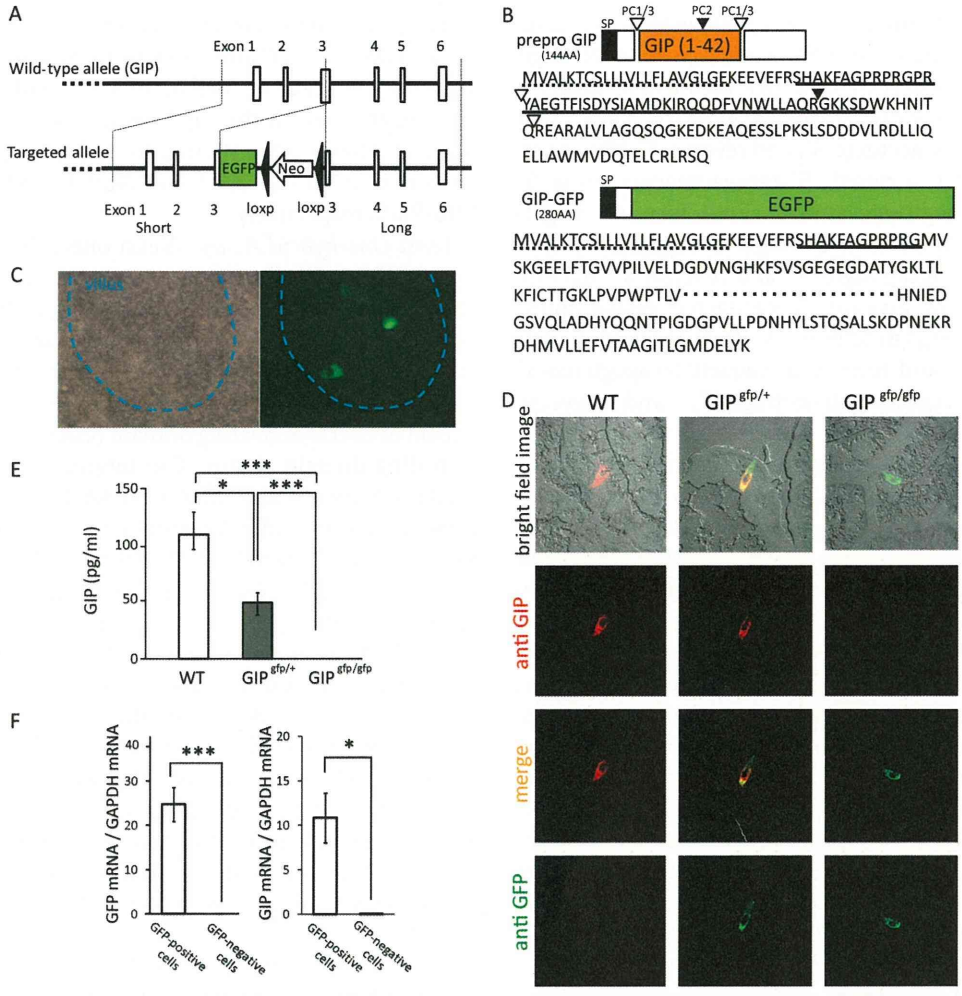

FIGURE 1. **Gene construct of GIP-GFP mice.** *A*, wild-type GIP allele and targeted allele of GIP-GFP. EGFP-poly(A)-loxp-Neo-loxp cassette was inserted into exon 3 of wild-type *gip* gene. *B*, prepro-GIP protein and GIP-GFP fusion protein. *SP*, signal peptide. *Open triangle*, PC1/3 cleavage site; *closed triangle*, PC2 cleavage site; *dotted line*, amino acids of signal peptide; *solid line*, translated protein from exon 3. *C*, microscopic images of upper small intestine in GIP-GFP heterozygous mice (bright field image and fluorescence image). *D*, immunohistochemical images of upper small intestine in wild-type (*WT*), GIP-GFP heterozygous ($GIP^{gfp/+}$), and homozygous mice ($GIP^{gfp/gfp}$). *Green*, GFP-expressing cells; *red*, GIP-expressing cells; *yellow*, merged image. *E*, fasting plasma GIP levels in WT, $GIP^{gfp/+}$, and $GIP^{gfp/gfp}$ mice. *F*, GFP mRNA and GIP mRNA levels in GFP-positive cells ($n = 5–6$) and GFP-negative cells ($n = 5–6$). *, $p \leq 0.05$; **, $p \leq 0.01$; ***, $p \leq 0.001$.

(280 amino acids). GFP fluorescence was observed in the small intestine of GIP-GFP heterozygous mice (Fig. 1*C*) and GIP-GFP homozygous mice (data not shown).

Immunohistochemical analysis was performed to assess localization of GFP-expressing cells and GIP-expressing cells using anti-GFP and anti-GIP antibodies, respectively, in the upper small intestine of wild-type and GIP-GFP heterozygous and homozygous mice (Fig. 1*D*). GFP-expressing cells are present in the intestine of GIP-GFP heterozygous and homozygous mice and GIP-expressing cells are present in the intestine of both wild-type and GIP-GFP heterozygous mice. However, in GIP-GFP homozygous mice, no GIP-expressing cells were found. The GFP-expressing cells were identical to the GIP-expressing cells in the GIP-GFP heterozygous mice. We then examined the fasting plasma GIP levels in the three types of mice (Fig. 1*E*). GIP levels were significantly lower in GFP-GFP heterozygous mice compared with those in wild-type mice. GIP levels of GIP-GFP homozygous mice were not detectable. These results indicate that GIP-GFP heterozygous mice have only one normal *gip* gene and that GIP-GFP homozygous mice have no normal *gip* genes.

Next, GFP-positive cells were purified by a flow cytometry system. GFP-positive cells and GFP-negative cells from upper small intestinal epithelium of GIP-GFP heterozygous mice were separated and collected. GFP mRNA and GIP mRNA were highly expressed in GFP-positive cells (Fig. 1*F*). In microarray analysis, the expression levels of GIP mRNA were much higher in GFP-positive cells than those in GFP-negative cells (GFP-positive cells ($n = 3$) 12,951.55 ± 335.77 *versus* GFP-negative cells ($n = 3$) 1763.61 ±142.65; $p \leq 0.001$). These results demonstrate that the GFP-positive cells in the intestinal epithelium of GIP-GFP mice are K-cells.

Transcription Factor Rfx6 Is Expressed Exclusively in K-cells—Microarray analysis data revealed that mRNA of the transcription factor Rfx6 is highly expressed in GFP-positive cells (GFP-positive cells ($n = 3$) 2613.4 ± 341.9 *versus* GFP-negative cells ($n = 3$) 24.0 ± 6.7; $p \leq 0.05$). As seven members of the Rfx family were identified previously, we evaluated the expression

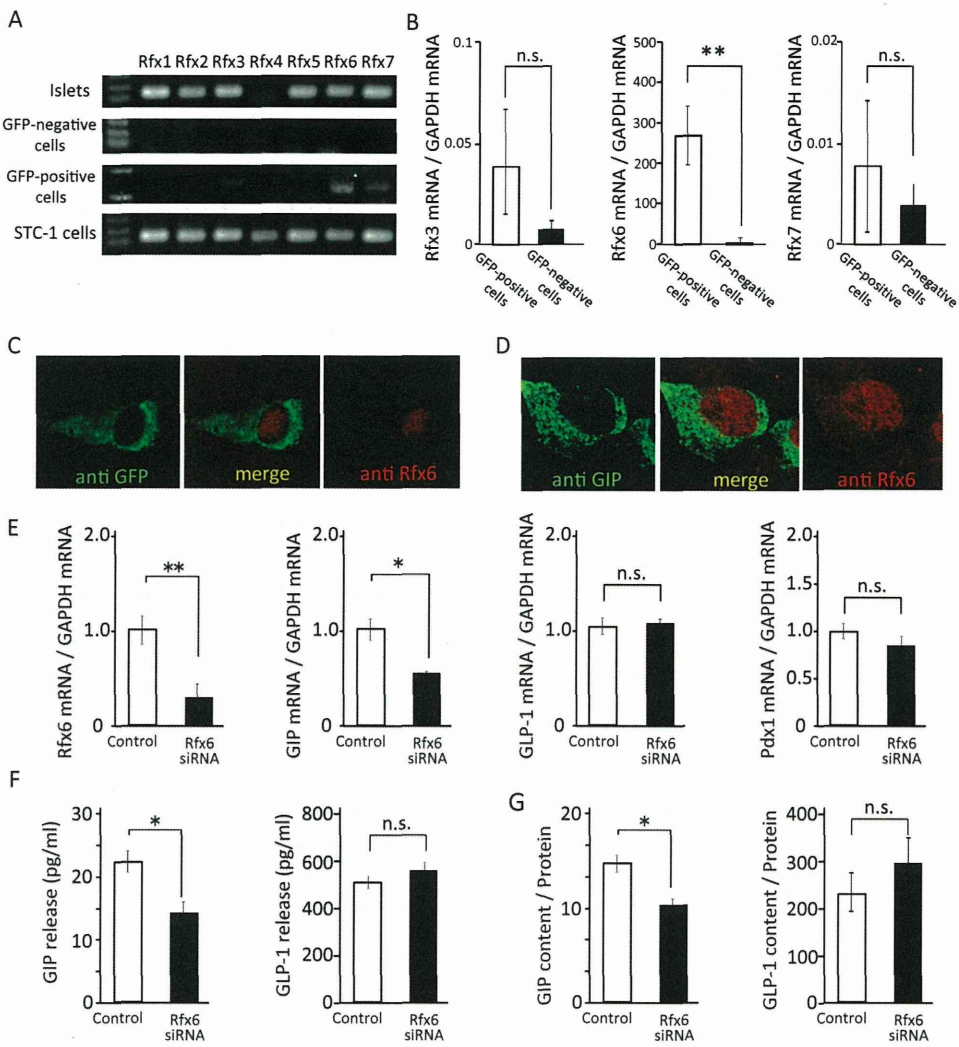

FIGURE 2. **Effect of Rfx6 on mRNA expression, cellular content, and secretion of GIP in STC-1 cells.** *A,* mRNA expression for *rfx* genes 1–7 in islets, GFP-negative cells, GFP-positive cells, and STC-1 cells by PCR. *B,* Rfx3, Rfx6, and Rfx7 mRNA levels in GFP-positive cells ($n = 8–10$) and GFP-negative cells ($n = 8–10$). *C,* immunohistochemical images of upper small intestine in GIP-GFP heterozygous mice. *Green,* GFP-expressing cells; *red,* Rfx6-expressing cells; *yellow,* merged image. *D,* immunohistochemical images of STC-1 cells. *Green,* GIP-expressing cells; *red,* Rfx6-expressing cells; *yellow,* merged image. *E,* Rfx6, GIP, GLP-1, and Pdx1 mRNA levels in Rfx6 knockdown STC-1 cells ($n = 4$). *F* and *G,* incretin content and secretion in Rfx6 knockdown STC-1 cells ($n = 4$). *, $p \leq 0.05$; **, $p \leq 0.01$, *n.s.*, not significant.

of these mRNAs in mouse islets, GFP-positive cells (K-cells), and mouse small intestinal cell line STC-1 (Fig. 2*A*). All of the *rfx* genes, except for *rfx4*, were expressed in islets as shown in a previous study (20). Rfx3, Rfx6, and Rfx7 were expressed in GFP-positive cells, but no Rfx mRNAs were detected in the GFP-negative cells. In semi-quantitative RT-PCR data, the expression levels of Rfx6 were extremely higher in GFP-positive cells than those in GFP-negative cells, whereas the expression levels of Rfx3 and Rfx7 were similar (Fig. 2*B*). Immunohistochemistry confirmed that Rfx6-expressing cells correspond to GFP-expressing cells (Fig. 2*C*), demonstrating that Rfx6 is expressed exclusively in K-cells.

Inhibition of Rfx6 and Pdx1 Expression Decreases GIP Expression in STC-1 Cells—We then assessed the influence of Rfx6 on GIP expression and secretion by using STC-1 cells. Rfx6 mRNA expression was confirmed in STC-1 cells by RT-PCR (Fig. 2*A*). The Rfx6-expressing cells were similarly located in the GIP-expressing cells by immunohistochemistry (Fig. 2*D*). By treatment with Rfx6 siRNA, Rfx6 mRNA expression was inhibited by 70% (Fig. 2*E*). In the same condition, mRNA expression, cellular content, and secretion of GIP were significantly decreased whereas those of GLP-1 were similar to control (Fig. 2, *E–G*), indicating that Rfx6 increases GIP mRNA expression, cellular content, and secretion. However, Pdx1 is reported to be an important transcriptional factor for producing GIP in K-cells (17, 18), although its expression levels were similar in GFP-positive and GFP-negative cells (Fig. 3*A*). To examine the effect of Pdx1 on incretin expression and secretion, mRNA expression, cellular content, and secretion of GIP and GLP-1 were measured in Pdx1-knockdown STC-1 cells by using siRNA. Pdx1 mRNA expression was confirmed in STC-1 cells by RT-PCR (Fig. 3*B*). The expression levels of Pdx1 mRNA were decreased by 50% in STC-1 cells treated with Pdx1 siRNA (Fig. 3*C*). GIP mRNA expression, cellular content, and secretion were significantly decreased, whereas GLP-1 mRNA expression, cellular content, and secretion were somewhat increased in STC-1 cells treated with Pdx1 siRNA (Fig. 3, *C–E*). The expression levels of Rfx6 mRNA were significantly decreased in the cells (Fig. 3*C*).

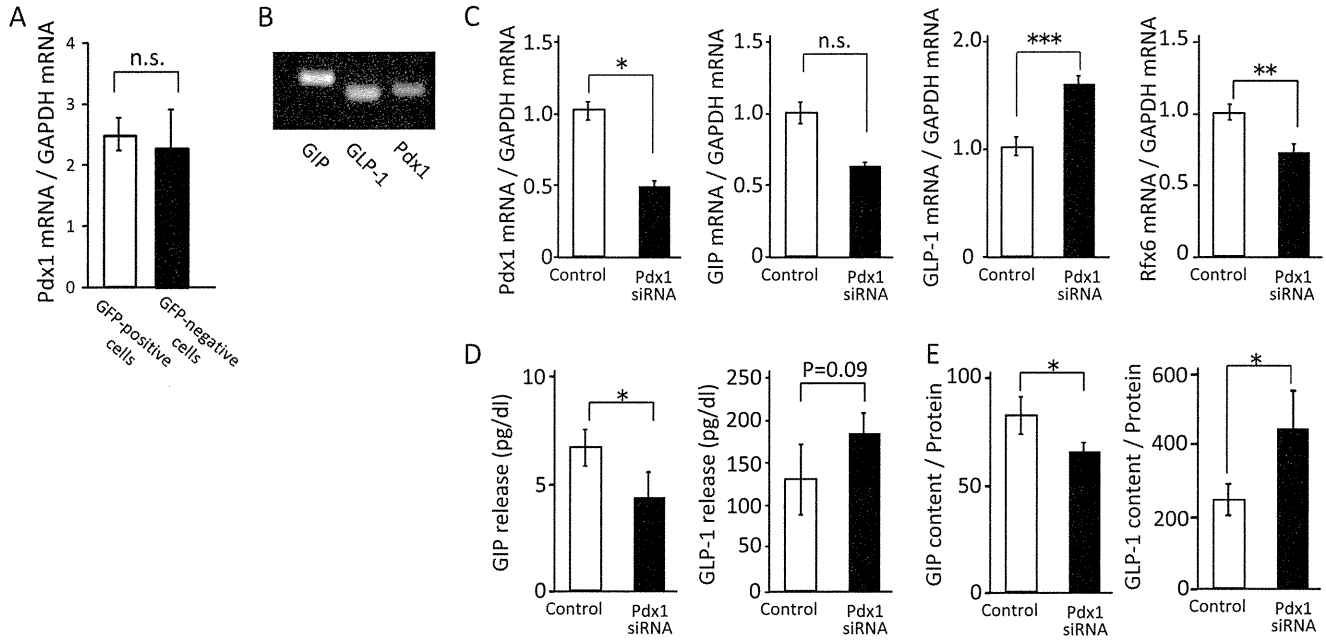

FIGURE 3. **Effect of Pdx1 on mRNA expression, cellular content, and secretion of GIP.** *A*, Pdx1 mRNA levels in GFP-positive cells and GFP-negative cells (n = 8–10). *B*, GIP, GLP-1, and Pdx1 mRNA expressions in STC-1 cells by RT-PCR. *C*, Pdx1, GIP, GLP-1, and Rfx6 mRNA levels in Pdx1 knockdown STC-1 cells (n = 4). *D* and *E*, incretin content and secretion in Pdx1 knockdown STC-1 cells (n = 4). *, $p \leq 0.05$; **, $p \leq 0.01$; ***, $p < 0.001$, *n.s.*, not significant.

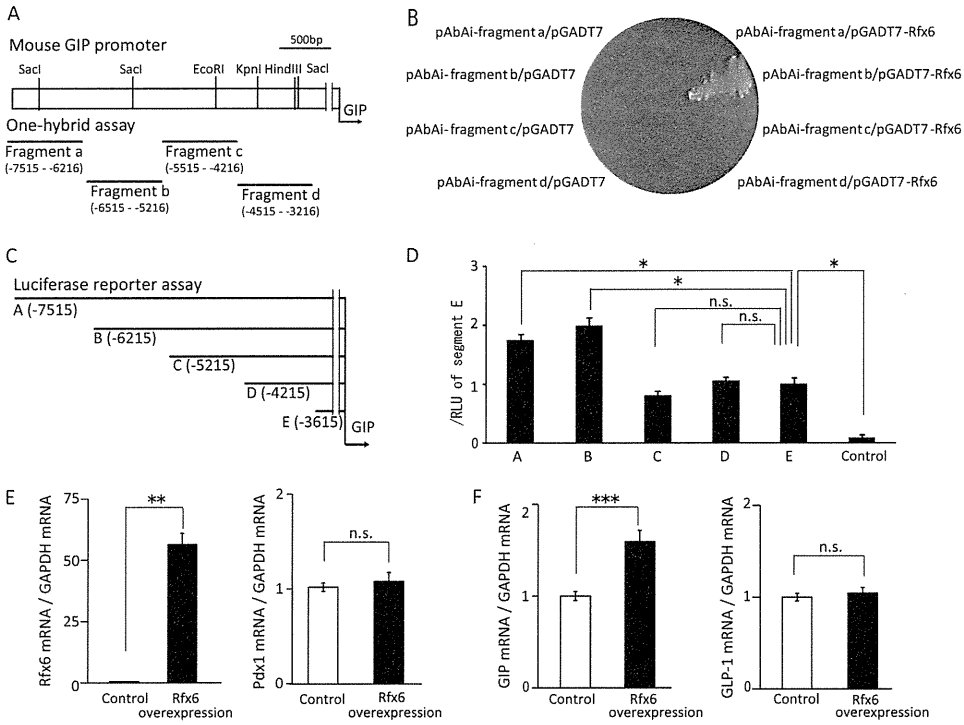

FIGURE 4. **Interaction of Rfx6 and *gip* gene.** *A*, design of the *gip* promoter fragments for one-hybrid assay. *Numbers* indicate nucleotides upstream from the transcription start site of the *gip* gene. *B*, results of yeast one-hybrid assay. Only yeast transformed with both pAbAi vector containing fragment b (*pAbAi-fragment b*) and Rfx6 cDNA-inserted pGADT7 (*pGADT7-Rfx6*) was grown on SD medium. *C*, design of the different lengths of *gip* promoter genes for luciferase reporter plasmid transfected in STC-1 cells. *D*, luciferase promoter assay on *gip* promoter. Data are represented by ratio of relative light units (*RLU*) of fragment E (n = 3–4). *, $p \leq 0.05$, *n.s.*, not significant. *E* and *F*, Pdx1, Rfx6, GIP, and GLP-1 mRNA levels in Rfx6-overexpressing STC-1 cells. **, $p \leq 0.01$; ***, $p \leq 0.001$ *versus* control, *n.s.*, not significant.

Interaction of Rfx6 and GIP Gene—We assessed the interaction of the Rfx6 and *gip* gene by one-hybrid assay. Four fragments of the *gip* promoter were constructed (Fig. 4*A*). Rfx6 effectively bound to fragment b (5216–6512 base pairs (bp) upstream of the *gip* promoter) (Fig. 4*B*). In the luciferase promoter assay, *gip* promoter activity of fragments A and B containing 5216–6512 bp upstream of *gip* promoter was high, whereas the activities of *gip* promoter C, D, and E were significantly decreased (Fig. 4*D*). These results suggest that Rfx6 binds to the region 5216–6512 bp upstream of the *gip* promoter,

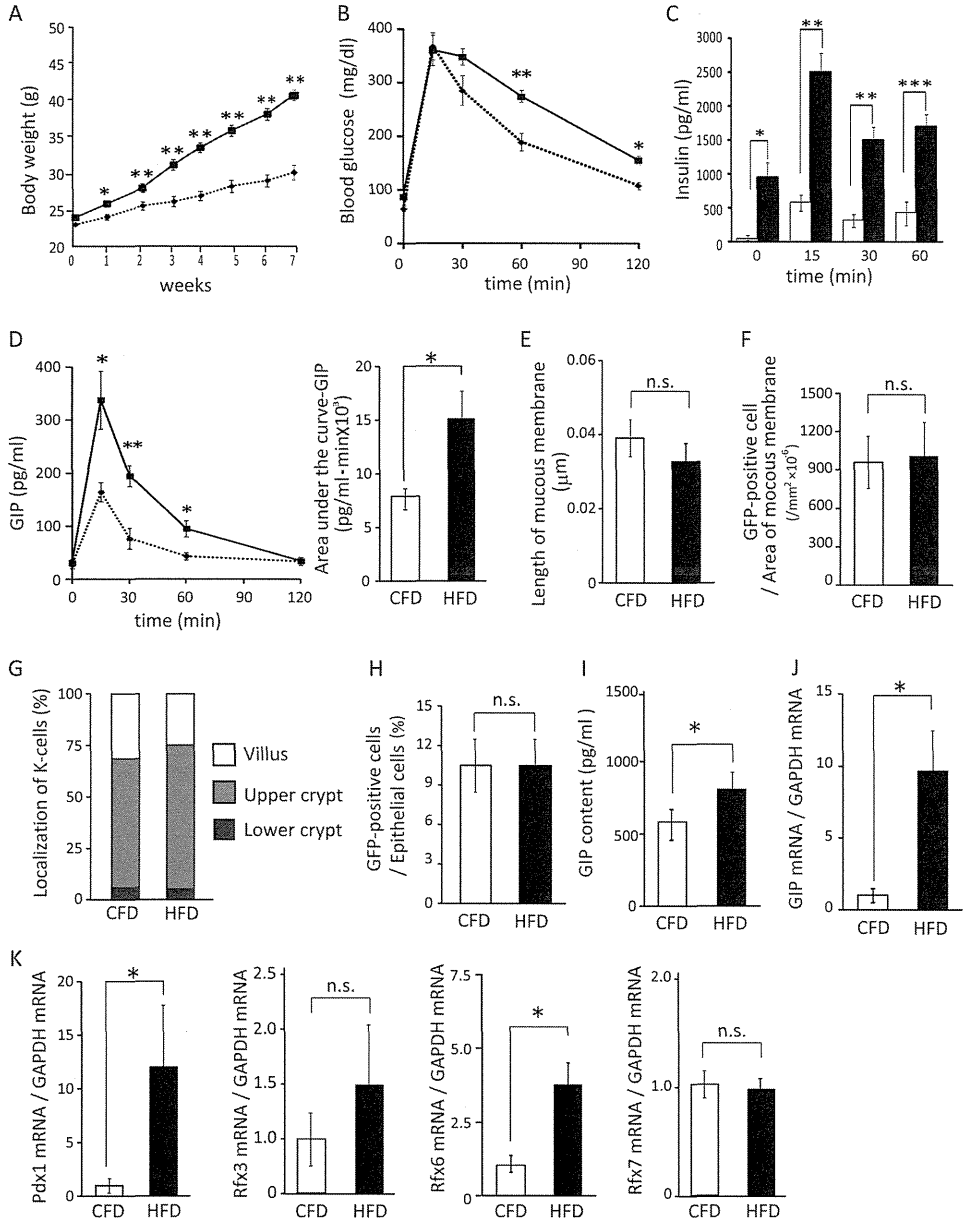

FIGURE 5. **Analysis of K-cells in the small intestine of CFD- and HFD-fed GIP-GFP heterozygous mice (histology, flow cytometry analysis, and gene expression).** *A,* body weight change of CFD-fed (*dashed line*) and HFD-fed (*continuous line*) GIP-GFP heterozygous mice (n = 5–7). *B–D,* blood glucose (*B*), insulin (*C*), and GIP levels (*D*) during OGTT after 8 weeks of CFD- or HFD-feeding (n = 5). *Dashed line* and *white box* shows CFD group, and *continuous line* and *black box* shows CFD group. *, $p \leq 0.05$; **, $p \leq 0.01$; ***, $p \leq 0.001$ *versus* CFD-fed mice. *E,* length of mucous membrane in upper small intestine (n = 5). *F,* number of GFP-positive cells by immunohistochemistry (n = 5). *G,* localization of K-cells in the upper small intestine by immunohistochemistry (n = 5). *H,* number of K-cells in the upper small intestine by flow cytometry analysis (n = 5). *I,* GIP content in upper small intestine (n = 5–7). *J,* GIP mRNA levels in GFP-positive cells (n = 8–10). *K,* Pdx1, Rfx3, Rfx6, and Rfx7 mRNA levels in GFP-positive cells (n = 8–10). *, $p \leq 0.05$; *n.s.*, not significant.

which regulates the *gip* promoter activity. Furthermore, Rfx6 was overexpressed in STC-1 cells by transfection of Rfx6 expression plasmids. The expression levels of Rfx6 mRNA levels were significantly higher in Rfx6-overexpressing cells compared with control (Fig. 4*E*). Rfx6 had no effect on the expression levels of to Pdx1 mRNA. GIP mRNA expression levels were significantly increased in Rfx6-overexpressing cells, but GLP-1 mRNA expression levels were not (Fig. 4*F*).

HFD Feeding Increases GIP Secretion and Induces Obesity and Insulin Hypersecretion in GIP-GFP Heterozygous Mice—To investigate the mechanisms of GIP hypersecretion in HFD-induced obesity *in vivo*, GIP-GFP heterozygous mice were fed CFD or HFD for 8 weeks. One week after starting these diets, the body weight of the HFD group was significantly increased compared with that of the CFD group (Fig. 5*A*). There was no difference in food and water intake between the CFD and HFD groups (data not shown). After CHD or HFD feeding for 8 weeks, OGTTs were performed. Blood glucose levels were significantly increased at 60 and 120 min during OGTT in HFD group (Fig. 5*B*). Insulin levels also were significantly increased in the HFD group (Fig. 5*C*). Insulin secretion (area under the curve-insulin) of the HFD group was increased about 5.5-fold compared with that of the CFD group (CFD group (n = 6) 38,221 ± 238 *versus* HFD group (n = 6) 211,835 ± 456; $p \leq$

0.001). GIP concentrations of HFD group at 15, 30, and 60 min were increased significantly compared with those of the CFD group (Fig. 5*D*). GIP secretion (area under the curve-GIP) of the HFD group was increased about 1.5-fold compared with that of the CFD group (CFD group (n = 6) 7368 ± 123 *versus* HFD group (n = 6) 10,531 ± 216; $p \leq 0.05$) These results show that HFD feeding increases GIP secretion and induces obesity and insulin hypersecretion in GIP-GFP heterozygous mice, which have only one normal *gip* gene.

GIP Hypersecretion in HFD-induced Obese Mice Is Not Due to Increase of K-cell Number but to Increase of GIP Expression in K-cells—To determine whether GIP hypersecretion involves an increased number of K-cells in HFD-fed GIP-GFP heterozygous mice, the number and localization of the K-cells in the upper small intestine were estimated and compared. The length of the mucous membrane and the number and localization of K-cells examined by immunohistochemistry were similar in the CFD and HFD group (Fig. 5, *E–G*). Flow cytometry analysis also showed no difference in K-cell number between the two groups (Fig. 5*H*). However, GIP content in the upper small intestine was significantly increased in the HFD group compared with that in the CFD group (Fig. 5*I*). In addition, in K-cells purified using flow cytometry, the expression levels of GIP mRNA were almost 10-fold higher in the HFD group than those in the CFD group (Fig. 5*J*). These results demonstrate that GIP hypersecretion under HFD-induced obesity is not due to an increase in K-cell number but to an increase of GIP mRNA expression and content in K-cells.

Rfx6 and Pdx1 mRNA Levels Were Increased in K-cells of HFD-induced Obese Mice—We also assessed the expression of other candidate genes in K-cells (GFP-positive cells) (Fig. 5*K*) and non-K-cells (GFP-negative cells). Both Rfx6 and Pdx1 mRNA levels were increased in K-cells of the HFD group compared with those in K-cells of the CFD group, but the mRNA expression levels of Rfx3 and Rfx7 were not. Other Rfx transcriptional factors (Rfx1, -2, -4, and -5) were not detected in the K-cells of HFD-fed mice. Furthermore, none of the Rfx transcriptional factors were detected in non-K-cells. Pdx1 mRNA expression was detected in non-K-cells, but there was no significant difference in the expression level between the CHD group and the HFD group (ratio of Pdx1 mRNA to GAPDH mRNA: CFD group (n = 8) 0.47 ± 0.15 *versus* HFD group (n = 8) 0.26 ± 0.08; p = 0.24). These results strongly suggest that an increase in Rfx6 expression as well as Pdx1 expression in K-cells stimulates GIP mRNA expression and content in K-cells of HFD-fed obese mice.

DISCUSSION

Analysis of K-cells *in vivo* has been impossible due to the inability to isolate the GIP-producing K-cells from intestinal epithelium. In this study, GIP-GFP mice enabled sorting GFP-positive cells as K-cells and revealed that the transcription factor Rfx6 is expressed exclusively in K-cells by microarray analysis and RT-PCR (Fig. 2*B*). Rfx3 and Rfx7 also were detected in K-cells by RT-PCR, but there were no significant differences in their expression between K-cells and non-K-cells (Fig. 2*B*). The *rfx* gene family of transcription factors was first detected in mammals as regulatory factors that bind to the promoter regions of major histocompatibility complex (*MHC*) class II genes (21); seven types of Rfx (Rfx1–7) have so far been identified. All Rfx transcription factors have a winged helix DNA binding domain. Rfx1–4 and -6 have a dimerization domain (22, 23), and Rfx6 forms homodimers or heterodimers with Rfx2 or Rfx3 (24, 25). Rfx6 was initially isolated from human genome sequences in 2008 (22). Serial Analysis of Gene Expression (SAGE) frequency data showed high expression of Rfx6 mRNA in the pancreas, liver, and heart, and RT-PCR analysis showed high expression of Rfx6 mRNA in human pancreas and intestine (20). However, it is known that Rfx3 mRNA is expressed in brain, placenta, pancreas, and pituitary and that Rfx3 directly regulates the promoters of *glut2* and glucokinase in pancreatic β-cells (26). Rfx7 is known to be expressed in many different tissues. *rfx3*- and *rfx6*-deficient mice were generated previously, and none of the endocrine cells, excluding pancreatic polypeptide-expressing cells, are detected in the islets of these mice (20, 27). These results suggest that Rfx3 and Rfx6 play a critical role in generating the endocrine cells in islets, but it is unknown whether they are associated with generation of enteroendocrine cells such as K-cells and L-cells. We examined incretin mRNA expression and content under the inhibition of Rfx6 expression in STC-1 cells. Other incretin GLP-1 mRNA expression and content were preserved in Rfx6-knockdown STC-1 cells. However, GIP mRNA expression and content were significantly decreased in the cells (Fig. 2, *E–G*). In addition, Rfx3 expression tended to be higher in GFP-positive cells than that in GFP-negative cells (Fig. 2*B*), but GIP mRNA expression, content, and secretion were not changed in Rfx3-knockdown STC-1 cells (data not shown). These results suggest that Rfx6 expressed exclusively in K-cells plays an important role in GIP expression, cellular content, and secretion in K-cells. In addition, we examined the effect of Rfx6 on the *gip* gene and found that Rfx6 binds to the region 5216–6512 bp upstream of the *gip* promoter gene (Fig. 4*D*) and that Rfx6 increased GIP mRNA expression in STC-1 cells (Fig. 4*F*). Further study is needed to clarify the regulatory mechanism of *gip* promoter activity by Rfx6. In previous studies, characterization of K-cells and microarray analysis were done using purified K-cells from the intestine of transgenic mice expressing a yellow fluorescent protein (YFP) under the control of the 200-kb rat *gip* promoter (28, 29), but Rfx6 expression in K-cells was not reported. The reason such a long promoter is required for specific expression of YFP in K-cells is not known, but it suggests that regulation of *gip* gene expression is under complex control. In this study, we established GIP-GFP mice in which GFP is under an endogenous native promoter. Using these GIP-GFP mice, we were able to determine that Rfx6 is expressed exclusively in K-cells.

In previous studies, Pdx1 expression was detected in K-cells, and *pdx1*-deficient mice showed a greatly decreased number of GIP-expressing cells in the intestine (18, 19). It also has been reported that Pdx1 binds 150 bp upstream of the *gip* promoter, activates the *gip* promoter in STC-1 cells, and that Pdx1 expression is essential for producing GIP in K-cells (18, 19). We found that there was no significant difference in Pdx1 mRNA expression between upper small intestinal K-cells and non-K-cells (Fig. 3*A*). These findings suggest the possibility that Rfx6 spe-

cifically expressed in K-cells plays a critical role in differentiation and GIP production of K-cells in collaboration with Pdx1. It was reported that Rfx6 mRNA expression is regulated by transcription factor neurogenin 3 (Ngn3) in the pancreas of the mouse fetus (30). In another report, no colocalization of Pdx1-expressing cells and Rfx6-expressing cells was found in pancreas of the mouse fetus using immunohistochemistry analysis, and Pdx-1 expression was decreased in the pancreas of Rfx6-deficient mice (20). In this study, Pdx1 mRNA expression levels were changed not only in Rfx6-knockdown STC-1 cells but also in Rfx6-overexpressing STC-1 cells, whereas Rfx6 expression levels were significantly decreased in Pdx1 knockdown STC-1 cells (Figs. 2*E*, 3*C*, and 4*E*). These results suggest that Rfx6 expression is regulated at least in part by Pdx1.

Increased blood GIP levels in obesity have been reported in several studies (7, 14–16). There is a report that healthy human subjects administered high fat food for 2 weeks showed increased plasma GIP levels without developing obesity, suggesting that GIP hypersecretion precedes obesity (31). GIP is released from K-cells into the circulation in response to various nutrients (32–34). Measurement of total GIP and total GLP-1 levels in humans challenged with glucose or meal shows that the postprandial plasma GIP level is greatly augmented when a meal containing abundant fat rather than simple glucose is consumed (35, 36). This suggests that intake of HFD increases GIP secretion and strengthens both direct and indirect effects of GIP on energy accumulation in adipose tissue. We previously reported that both GIP levels after glucose loading and body mass index have a positive correlation in healthy subjects (37). In this study, GIP levels during OGTT were increased in obese GIP-GFP heterozygous mice compared with those in lean GIP-GFP heterozygous mice, even though GIP-GFP heterozygous mice have only one normal *gip* gene, indicating these mice represent a useful model for analysis of the mechanisms involved in the augmented GIP secretion in HFD-induced obesity. A previous study reported that augmentation of GIP secretion in HFD feeding conditions is due to increased K-cell number (38). In that report, agglomerates of Pdx1 and GIP double-expressing cells were found inside the duodenal mucosa of obese rats after HFD feeding. In this study, however, we could not detect agglomerates of K-cells or an increase of K-cell number in the duodenum or upper small intestine of HFD-fed GIP-GFP heterozygous mice by immunohistochemistry and flow cytometry analysis. The reason for this discrepancy could be the difference of species, food composition, and/or duration of the HFD feeding period. In our study, GIP content was significantly increased in the upper small intestine of HFD-fed mice compared with that in CFD-fed mice, and GIP mRNA expression was increased in K-cells of HFD-fed mice. These results suggest that GIP hypersecretion in HFD-induced obese mice is due to increased GIP expression in K-cells. In this condition, the expression levels of Rfx6 and Pdx1 mRNA were significantly increased in K-cells (Fig. 5*K*). As Rfx6 and Pdx1 were found to be important transcriptional factors in producing GIP in K-cells in our results using Rfx6 knockdown and overexpression and in previous *in vitro* studies for Pdx1, an increase in Rfx6 and Pdx1 expressions might well be involved in GIP hypersecretion in K-cells in HFD-induced obese mice.

In conclusion, gene analysis of K-cells isolated from GIP-GFP mice enables identification of the transcription factor Rfx6 that is expressed exclusively in K-cells and is involved in the regulation of GIP expression. We also show that expression of Rfx6 and Pdx1 is up-regulated in the K-cells of HFD-induced obese mice, which suggests that induction of Rfx6 as well as Pdx1 plays a critical role in GIP hypersecretion in HFD-induced obesity.

Acknowledgments—We thank Prof. Douglas Hanahan, University of California, San Francisco, for kindly providing the STC-1 cells. We also thank Dr. Yoshitaka Hayashi, Research Institute of Environmental Medicine, Nagoya University, for helpful suggestions regarding the study. Mouse anti-GIP antibody was kindly provided by Merck Millipore.

REFERENCES

1. Reaven, G. M. (1988) Banting lecture 1988. Role of insulin resistance in human disease. *Diabetes* **37,** 1595–1607
2. Kahn, B. B., and Flier, J. S. (2000) Obesity and insulin resistance. *J. Clin. Invest.* **106,** 473–481
3. Lemieux, I., Pascot, A., Couillard, C., Lamarche, B., Tchernof, A., Alméras, N., Bergeron, J., Gaudet, D., Tremblay, G., Prud'homme, D., Nadeau, A., and Després, J. P. (2000) Hypertriglyceridemic waist. A marker of the atherogenic metabolic triad (hyperinsulinemia; hyperapolipoprotein B; small, dense LDL) in men? *Circulation* **102,** 179–184
4. Pederson, R. A. (1994) in *Gut Peptides: Biochemistry and Physiology* (Walsh, J. H., and Dockray, G. J., eds) pp. 217–259, Raven Press, New York
5. Drucker, D. J. (1998) Glucagon-like peptides. *Diabetes* **47,** 159–169
6. Seino, Y., Fukushima, M., and Yabe, D. (2010) GIP and GLP-1, the two incretin hormone. Similarities and difference. *J. Diabetes Invest.* **1,** 8–23
7. Miyawaki, K., Yamada, Y., Ban, N., Ihara, Y., Tsukiyama, K., Zhou, H., Fujimoto, S., Oku, A., Tsuda, K., Toyokuni, S., Hiai, H., Mizunoya, W., Fushiki, T., Holst, J. J., Makino, M., Tashita, A., Kobara, Y., Tsubamoto, Y., Jinnouchi, T., Jomori, T., and Seino, Y. (2002) Inhibition of gastric inhibitory polypeptide signaling prevents obesity. *Nat. Med.* **8,** 738–742
8. Tsukiyama, K., Yamada, Y., Yamada, C., Harada, N., Kawasaki, Y., Ogura, M., Bessho, K., Li, M., Amizuka, N., Sato, M., Udagawa, N., Takahashi, N., Tanaka, K., Oiso, Y., and Seino, Y. (2006) Gastric inhibitory polypeptide as an endogenous factor promoting new bone formation following food ingestion. *Mol. Endocrinol.* **20,** 1644–1651
9. Miyawaki, K., Yamada, Y., Yano, H., Niwa, H., Ban, N., Ihara, Y., Kubota, A., Fujimoto, S., Kajikawa, M., Kuroe, A., Tsuda, K., Hashimoto, H., Yamashita, T., Jomori, T., Tashiro, F., Miyazaki, J., and Seino, Y. (1999) Glucose intolerance caused by a defect in the entero-insular axis. A study in gastric inhibitory polypeptide receptor knockout mice. *Proc. Natl. Acad. Sci. U.S.A.* **96,** 14843–14847
10. Harada, N., Yamada, Y., Tsukiyama, K., Yamada, C., Nakamura, Y., Mukai, E., Hamasaki, A., Liu, X., Toyoda, K., Seino, Y., and Inagaki, N. (2008) A novel GIP receptor splice variant influences GIP sensitivity of pancreatic beta-cells in obese mice. *Am. J. Physiol. Endocrinol. Metab.* **294,** E61–E68
11. Usdin, T. B., Mezey, E., Button, D. C., Brownstein, M. J., and Bonner, T. I. (1993) Gastric inhibitory polypeptide receptor, a member of the secretin-vasoactive intestinal peptide receptor family, is widely distributed in peripheral organs and the brain. *Endocrinology* **133,** 2861–2870
12. Hauner, H., Glatting, G., Kaminska, D., and Pfeiffer, E. F. (1988) Effects of gastric inhibitory polypeptide on glucose and lipid metabolism of isolated rat adipocytes. *Ann. Nutr. Metab.* **32,** 282–288
13. Song, D. H., Getty-Kaushik, L., Tseng, E., Simon, J., Corkey, B. E., and Wolfe, M. M. (2007) Glucose-dependent insulinotropic polypeptide enhances adipocyte development and glucose uptake in part through Akt activation. *Gastroenterology* **133,** 1796–1805
14. Bailey, C. J., Flatt, P. R., Kwasowski, P., Powell, C. J., and Marks, V. (1986) Immunoreactive gastric inhibitory polypeptide and K cell hyperplasia in

obese hyperglycaemic (ob/ob) mice fed high fat and high carbohydrate cafeteria diets. *Acta Endocrinol.* **112,** 224–229
15. Flatt, P. R., Bailey, C. J., Kwasowski, P., Swanston-Flatt, S. K., and Marks, V. (1983) Abnormalities of GIP in spontaneous syndromes of obesity and diabetes in mice. *Diabetes* **32,** 433–435
16. Creutzfeldt, W., Ebert, R., Willms, B., Frerichs, H., and Brown, J. C. (1978) Gastric inhibitory polypeptide (GIP) and insulin in obesity. Increased response to stimulation and defective feedback control of serum levels. *Diabetologia* **14,** 15–24
17. Jonsson, J., Carlsson, L., Edlund, T., and Edlund, H. (1994) Insulin-promoter-factor 1 is required for pancreas development in mice. *Nature* **371,** 606–609
18. Jepeal, L. I., Fujitani, Y., Boylan, M. O., Wilson, C. N., Wright, C. V., and Wolfe, M. M. (2005) Cell-specific expression of glucose-dependent-insulinotropic polypeptide is regulated by the transcription factor PDX-1. *Endocrinology* **146,** 383–391
19. Fujita, Y., Chui, J. W., King, D. S., Zhang, T., Seufert, J., Pownall, S., Cheung, A. T., and Kieffer, T. J. (2008) Pax6 and Pdx1 are required for production of glucose-dependent insulinotropic polypeptide in proglucagon-expressing L cells. *Am. J. Physiol. Endocrinol Metab.* **295,** E648–E657
20. Smith, S. B., Qu, H. Q., Taleb, N., Kishimoto, N. Y., Scheel, D. W., Lu, Y., Patch, A. M., Grabs, R., Wang, J., Lynn, F. C., Miyatsuka, T., Mitchell, J., Seerke, R., Désir, J., Vanden Eijnden, S., Abramowicz, M., Kacet, N., Weill, J., Renard, M. E., Gentile, M., Hansen, I., Dewar, K., Hattersley, A. T., Wang, R., Wilson, M. E., Johnson, J. D., Polychronakos, C., and German, M. S. (2010) Rfx6 direct islet formation and insulin production in mice and humans. *Nature* **463,** 775–780
21. Reith, W., Barras, E., Satola, S., Kobr, M., Reinhart, D., Sanchez, C. H., and Mach, B. (1989) Cloning of the major histocompatibility complex class II promoter binding protein affected heredity defect in class II gene regulation. *Proc. Natl. Acad. Sci. U.S.A.* **86,** 4200–4204
22. Aftab, S., Semenec, L., Chu, J. S., and Chen, N. (2008) Identification and characterization of novel human tissue-specific RFX transcription factors. *BMC Evol. Biol.* **8,** 226–236
23. Katan-Khaykovich, Y., and Shaul, Y. (1998) RFX1, a single DNA-binding protein with a split dimerization domain, generates alternative complexes. *J. Biol. Chem.* **273,** 24504–24512
24. Rual, J. F., Venkatesan, K., Hao, T., Hirozane-Kishikawa, T., Dricot, A., Li, N., Berriz, G. F., Gibbons, F. D., Dreze, M., Ayivi-Guedehoussou, N., Klitgord, N., Simon, C., Boxem, M., Milstein, S., Rosenberg, J., Goldberg, D. S., Zhang, L. V., Wong, S. L., Franklin, G., Li, S., Albala, J. S., Lim, J., Fraughton, C., Llamosas, E., Cevik, S., Bex, C., Lamesch, P., Sikorski, R. S., Vandenhaute, J., Zoghbi, H. Y., Smolyar, A., Bosak, S., Sequerra, R., Doucette-Stamm, L., Cusick, M. E., Hill, D. E., Roth, F. P., and Vidal, M. (2005) Towarda proteome-scale map of the human protein-protein interaction network. *Nature* **437,** 1173–1178
25. Rhodes, D. R., Tomlins, S. A., Varambally, S., Mahavisno, V., Barrette, T., Kalyana-Sundaram, S., Ghosh, D., Pandey, A., and Chinnaiyan, A. M. (2005) Probabilistic model of the human protein-protein interaction network. *Nat. Biotechnol.* **23,** 951–959
26. Ait-Lounis, A., Bonal, C., Seguín-Estévez, Q., Schmid, C. D., Bucher, P., Herrera, P. L., Durand, B., Meda, P., and Reith, W. (2010) The transcription factor Rfx3 regulates beta-cell differentiation, function, and glucokinase expression. *Diabetes* **59,** 1674–1685
27. Ait-Lounis, A., Baas, D., Barras, E., Benadiba, C., Charollais, A., Nlend Nlend, R., Liègeois, D., Meda, P., Durand, B., and Reith, W. (2007) Novel function of ciliogenic transcription factor RFX3 in development of the endocrine pancreas. *Diabetes* **56,** 950–959
28. Parker, H. E., Habib, A. M., Rogers, G. J., Gribble, F. M., and Reimann, F. (2009) Nutrient-dependent secretion of glucose-dependent insulinotropic polypeptide from primary murine K cells. *Diabetologia* **52,** 289–298
29. Habib, A. M., Richards, P., Cairns, L. S., Rogers, G. J., Bannon, C. A., Parker, H. E., Morley, T. C., Yeo, G. S., Reimann, F., and Gribble, F. M. (2012) Overlap of endocrine hormone expression in the mouse intestine revealed by transcriptional profiling and flow cytometry. *Endocrinology* **153,** 3054–3065
30. Soyer, J., Flasse, L., Raffelsberger, W., Beucher, A., Orvain, C., Peers, B., Ravassard, P., Vermot, J., Voz, M. L., Mellitzer, G., and Gradwohl, G. (2010) Rfx6 is an Ngn3-dependent winged helix transcription factor required for pancreatic islet cell development. *Development* **137,** 203–212
31. Brøns, C., Jensen, C. B., Storgaard, H., Hiscock, N. J., White, A., Appel, J. S., Jacobsen, S., Nilsson, E., Larsen, C. M., Astrup, A., Quistorff, B., and Vaag, A. (2009) Impact of short-term high fat feeding on glucose and insulin metabolism in young healthy men. *J. Physiol.* **587,** 2387–2397
32. Yoder, S. M., Yang, Q., Kindel, T. L., and Tso, P. (2010) Differential responses of the incretin hormones GIP and GLP-1 to increasing doses of dietary carbohydrate but not dietary protein in lean rats. *Am. J. Physiol. Gastrointest. Liver Physiol.* **299,** G476–G485
33. Brown, J. C., Dryburgh, J. R., Ross, S. A., and Dupré, J. (1975) Identification and actions of gastric inhibitory polypeptide. *Recent Prog. Horm. Res.* **31,** 487–532
34. Falko, J. M., Crockett, S. E., Cataland, S., and Mazzaferri, E. L. (1975) Gastric inhibitory polypeptide (GIP) stimulated by fat ingestion in man. *J. Clin. Endocrinol. Metab.* **41,** 260–265
35. Vollmer, K., Holst, J. J., Baller, B., Ellrichmann, M., Nauck, M. A., Schmidt, W. E, and Meier, J. J. (2008) Predictors of incretin concentrations in subjects with normal, impaired, and diabetic glucose tolerance. *Diabetes* **57,** 678–687
36. Yamane, S., Harada, N., Hamasaki, A., Muraoka, A., Joo, E., Suzuki, K., Nasteska, D., Tanaka, D., Ogura, M., Harashima, S., and Inagaki, N. (2012) Effects of glucose and meal ingestion on incretin secretion in Japanese subjects with normal glucose tolerance. *J. Diabetes Invest.* **3,** 81–85
37. Harada, N., Hamasaki, A., Yamane, S., Muraoka, A., Joo, E., Fujita, K., and Inagaki, N. (2011) Plasma GIP and GLP-1 levels are associated with distinct factors after glucose loading in Japanese subjects. *J. Diabetes Invest.* **2,** 193–199
38. Gniuli, D., Calcagno, A., Dalla Libera, L., Calvani, R., Leccesi, L., Caristo, M. E., Vettor, R., Castagneto, M., Ghirlanda, G., and Mingrone, G. (2010) High-fat feeding stimulates endocrine, glucose-dependent insulinotropic polypeptide (GIP)-expressing cell hyperplasia in the duodenum of Wistar rats. *Diabetologia* **53,** 2233–2240

Molecular Genetics and Metabolism 109 (2013) 112–117

Contents lists available at SciVerse ScienceDirect

Molecular Genetics and Metabolism

journal homepage: www.elsevier.com/locate/ymgme

Exome sequencing identifies a new candidate mutation for susceptibility to diabetes in a family with highly aggregated type 2 diabetes

Daisuke Tanaka [a], Kazuaki Nagashima [a], Mayumi Sasaki [a], Shogo Funakoshi [a], Yasushi Kondo [a], Koichiro Yasuda [b], Akio Koizumi [c], Nobuya Inagaki [a,*]

[a] Department of Diabetes and Clinical Nutrition, Graduate School of Medicine, Kyoto University, 54 Shogoin-Kawahara-cho, Sakyo-ku, Kyoto, 606-8507, Japan
[b] Saiseikai Noe Hospital, 1-3-25 Furuichi, Joto-ku, Osaka, 536-0001, Japan
[c] Department of Health and Environmental Sciences, Graduate School of Medicine, Kyoto University, Yoshidakonoe-cho, Sakyo-ku, Kyoto, 606-8501, Japan

ARTICLE INFO

Article history:
Received 15 January 2013
Received in revised form 13 February 2013
Accepted 13 February 2013
Available online 21 February 2013

Keywords:
Genetics of type 2 diabetes
Linkage analysis
Exome sequencing
EEA1

ABSTRACT

The aim of this study was to investigate the genetic background of familial clustering of diabetes using genome-wide linkage analysis combined with exome sequencing. We recruited a Japanese family with a 3-generation history of diabetes. The family comprised 16 members, 13 having been diagnosed with diabetes. Nine members had been diagnosed before the age of 40. Linkage analysis was performed assuming an autosomal dominant model. Linkage regions were observed on chromosomes 4q34, 5q11–q13, and 12p11–q22 and the logarithm of odds (LOD) scores were 1.80. To identify the susceptibility variants, we performed exome sequencing of an affected family member. We predicted that the familial clustering of diabetes is caused by a rare non-synonymous variant, and focused our analysis on non-synonymous variants absent in dbSNP131. Exome sequencing identified 10 such variants in the linkage regions, 7 of which were concordant with the affection status in the family. One hundred five normal subjects and 67 lean diabetes subjects were genotyped for the 7 variants; the only variant found to be significantly more frequent in the diabetes subjects than in the normal subjects was the N1072K variant of the early endosome antigen 1 (EEA1) gene (0 in normal subjects and 4 in diabetes subjects, $p = 0.022$). We therefore propose that the N1072K variant of the EEA1 gene is a candidate mutation for susceptibility to diabetes in the Japanese population.

1. Introduction

In Japan, 11.2% of all adults suffer from diabetes mellitus, and its increasing prevalence is a serious concern [1]. Most of these patients have type 2 diabetes. While recent advances in genome-wide association studies (GWAS) have revealed over 60 type 2 diabetes susceptibility loci, all of them account for less than 20% of the genetic background of the disease [2–4]. GWAS is based on the common disease-common variant hypothesis, and rare disease variants with large effect size are frequently missed [5]. Approaches other than GWAS are necessary to elucidate the greater part of the genetic background of type 2 diabetes.

A family-based study is a promising approach to identify rare disease variants with large effect size [6]. Familial clustering of diabetes is frequently observed and the typical example of familial diabetes caused by rare disease variants is Maturity Onset Diabetes of the Young (MODY). However, in most families in Japan, familial clustering cannot be attributed to mutations of the known 6 MODY genes (*HNF4A*, *GCK*, *HNF1A*, *PDX1*, *HNF1B*, and *NEUROD1*) despite intensive linkage analyses and candidate-gene screening [7,8], and the genetic predisposition in such families has not been ascertained.

Recently, exome sequencing has become a powerful strategy for identifying causative genes for a number of Mendelian disorders [9]. As exome sequencing identifies thousands of exonic variants, a selection strategy to identify the particular variant causing the disorder is necessary.

In the present study, we combined linkage analysis and exome sequencing to identify the causal genetic variant in a family with highly aggregated diabetes and elucidated the genetic background of type 2 diabetes in Japan.

2. Material and methods

2.1. Family members

We recruited a Japanese family with a 3-generation family history of diabetes mellitus (Fig. 1). Medical history was gained from the family members and body mass index (BMI) and HbA_{1c} levels were measured in the year 2010 at entry to the study. All study participants

Abbreviations: LOD, Logarithm of Odds; EEA1, Early Endosome Antigen 1; GWAS, Genome-Wide Association Study; MODY, Maturity Onset Diabetes of the Young; HNF4A, Hepatocyte Nuclear Factor 4 Alpha; BMI, Body Mass Index; SNP, Single Nucleotide Polymorphism; CNV, Copy Number Variation; MAF, Minor Allele Frequency.

* Corresponding author. Fax: +81 75 771 6601.
E-mail address: inagaki@metab.kuhp.kyoto-u.ac.jp (N. Inagaki).

1096-7192/$ – see front matter © 2013 Elsevier Inc. All rights reserved.
http://dx.doi.org/10.1016/j.ymgme.2013.02.010

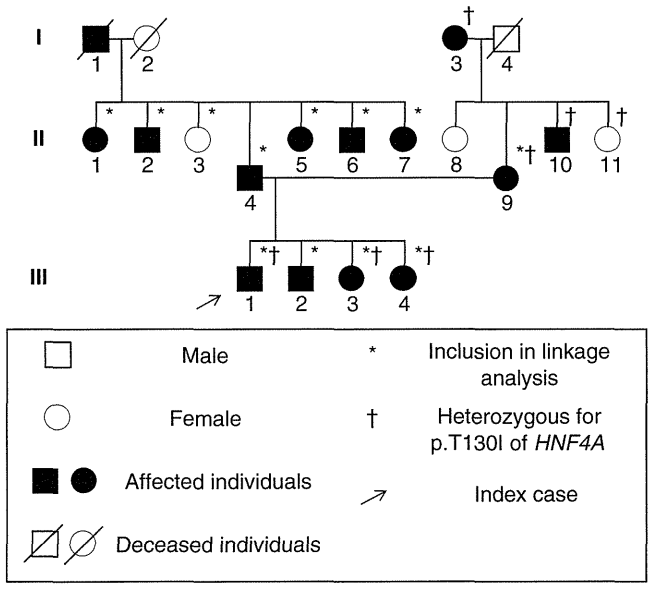

Fig. 1. A pedigree with familial aggregated diabetes mellitus.

from the family were negative for glutamic acid decarboxylase antibody. Affected status of the participants was determined in two ways. First, if participants had been diagnosed with diabetes and treated with oral antidiabetic drugs or insulin injection, they were regarded as affected. Second, if participants had not been treated with oral antidiabetic drugs or insulin injection, they underwent HbA_{1c} measurement. If their HbA_{1c} levels were $\geq$6.5% [10], they were also regarded as affected. The clinical features of family members are shown in Table 1.

Deceased individual I-1 had diabetes according to the interview with family members. There was no information suggesting consanguineous marriage in the family. Some of the individuals in generation II had offspring and none of them except III-1, 2, 3, and 4, had diabetes according to the information from family members.

2.2. Normoglycemic controls and diabetes subjects

We selected normoglycemic controls from the participants in an annual medical check-up program performed in Japan. Nine-hundred ninety local residents (430 men, 560 women) were recruited in the program and consented to donate their DNA. From 2002 to 2007, participants underwent physical examination and blood tests including fasting plasma glucose and HbA_{1c} every year. Subjects defined as normoglycemic controls had the following characteristics: both HbA_{1c} and fasting plasma glucose below the screening standards for the diagnosis of diabetes (HbA_{1c}<6.0% and fasting plasma glucose<5.5 mmol/l [10]) during 5-year follow-up span, and age$\geq$55. The number of subjects that satisfied the definition was 206 (81 men, 125 women). For genotyping, 105 normoglycemic controls were randomly selected (Supplementary Table 1), because genotyping of 210 normal chromosomes is necessary to achieve 80% power to detect a polymorphism present in 1% of the population [11]. We recruited lean diabetes subjects from participants in another medical check-up program performed in Japan. One hundred and thirty-eight participants had been diagnosed with diabetes and 68 were lean (BMI<25). DNA was available from 67 of the lean diabetes subjects (Supplementary Table 1). Another, unrelated 64 diabetes subjects with family history had visited collaborating hospitals in Japan and donated their DNA. Genomic DNA was extracted from blood samples with a QIAamp DNA Blood Mini kit (Qiagen).

Table 1
Characteristics of the family members.

ID	Age	Sex	BMI	HbA_{1c} (%)	Age when diagnosed	Current therapy
I-3	88	F	16.8	5.6	N/A	Oral drug
II-1	78	F	23.8	6.8	35	Oral drug
II-2	75	M	22.7	7.5	35	Oral drug
II-3	72	F	28.2	6.0		
II-4	68	M	23.3	9.2	35	Oral drug
II-5	65	F	24.6	6.8	65	Diet
II-6	62	M	22.4	8.1	30	Diet
II-7	60	F	23.3	7.6	35	Insulin 10 U/d
II-8	68	F	26.7	5.7		
II-9	66	F	23.9	7.8	44	Oral drug
II-10	63	M	20.5	7.4	N/A	Oral drug
II-11	61	F	21.2	5.4		
III-1	40	M	26.0	8.5	30	Oral drug
III-2	39	M	29.0	7.6	38	Oral drug
III-3	36	F	29.9	6.6	36	Diet
III-4	26	F	29.1	6.6	26	Diet

2.3. Linkage analysis

We performed a genome-wide linkage analysis using GENEHUNTER (version 2.1) software [12] with ABI Prism Linkage Mapping Set Version 2.5 (382 markers for 22 autosomes; Applied Biosystems) and other microsatellite fine markers designed according to information from the UniSTS map (http://www.ncbi.nlm.nih.gov/genome/sts/). A multipoint parametric linkage analyses for autosomes were performed assuming an autosomal dominant model because the 3-generation family history is suggestive of autosomal dominant mode of inheritance [6]. Since sensitivity analyses for the disease allele frequency by changing it from 0.01 to 0.00001 suggested negligible effects on LOD score, the disease allele frequency was set at 0.00001 and a phenocopy frequency of 0.00001 was assumed. Affected family members with known diabetes susceptibility variants were considered as having unknown phenotype. The purpose of including members assigned as unknown was to increase the accuracy of haplotype estimation in members assigned as affected, although inclusion did not increase the statistical power. Population allele frequencies for each microsatellite marker were assigned equal portions for individual alleles. We used a 2-stage design: first, all chromosomal regions were screened by genotyping at an approximately 10 cM density (screening), and the regions where LOD scores were highest were considered potentially interesting. Second, these regions were further finely mapped at approximately 1- to 2-cM densities (fine mapping). Haplotypes were constructed with GENEHUNTER.

2.4. Sanger sequencing

We directly sequenced the coding exons of 6 MODY genes (*HNF4A*, *GCK*, *HNF1A*, *PDX1*, *HNF1B*, and *NEUROD1*) by Sanger method. Forward and reverse PCR primers for each exon were selected in an intronic sequence 50 bp away from the intron/exon boundaries. PCR products were run on 2% agarose gel, and the appropriate bands were excised and then purified with the use of the QIAquick Gel Extraction Kit (Qiagen). Sequencing results were analyzed on an ABI 3130 genetic analyzer (Applied Biosystems). Sanger sequencing was also used to confirm the single nucleotide polymorphisms (SNPs) identified in exome sequencing. Sequencing primer data will be provided on request.

2.5. Copy number variation (CNV) analysis

We selected CNVs that overlapped with MODY genes (*HNF1A*, *HNF1B*, and *GCK*, Supplementary Table 2). We performed real-time PCR to determine CNV status on normal control and family members. TaqMan probes designed by the manufacturer (Applied Biosystems, Supplementary Table 2), were used to target the specific regions. *RNase P* (Taqman Copy Number Reference Assay, Applied Biosystems)

was chosen as a reference gene. Every reaction was triplicated. CopyCaller Software v2.0 (Applied Biosystems) was used to determine the copy number status of each target region.

2.6. Targeted capture and massive parallel sequencing

We conducted exome analysis on one affected family member who was negative for mutations in the exons of the 6 MODY genes. We targeted all protein-coding regions as defined by RefSeq37. Approximately 210,000 coding exons from 3 μg of genomic DNA were captured using the Agilent SureSelect Human All Exon 50 Mb kit, following the manufacturer's protocols. The whole-exome DNA library was sequenced on an Illumina Genome Analyzer IIx in 76-bp paired-end reads using two channels. Sequence reads were mapped to the reference human genome (Ghr37/hg19) using the Burrows-Wheeler Aligner (http://bio-bwa.sourceforge.net/). Variant detection was performed with the CASAVA software (version 1.7; Illumina). Calls of variants were filtered to include only those with ≥8× coverage, ≥40 consensus quality and ≥20 mapping quality.

2.7. Genotyping of SNPs

Genotyping of variants identified in the exome sequencing was performed in 105 normoglycemic controls and 67 lean diabetes subjects. The PCR-restriction fragment length polymorphism method for p.A80T of *CENPH*, p.R29C of *SREK1IP1*, and p.S33G of *SMAGP* and the Taqman method (Applied Biosystems) for p.F120L of *TMEM174*, p.P1818L of *NACA*, p.N1072K of *EEA1*, and p.E361G of *LRRIQ1* were used. Genotyping of the p.N1072K variant of *EEA1* was performed in another, unrelated 64 familial diabetes subjects.

2.8. RT-PCR analysis of the TMEM174 gene product in mouse tissues

Pancreatic islets and tissues of the lung, the heart, the liver and the kidney were obtained from C57BL/6 mice. Complementary DNA was prepared by reverse transcriptase (Invitrogen) with an oligo(dT) primer (Invitrogen). Messenger RNA expression was examined by PCR using the LA Taq (TaKaRa) and the oligonucleotide primers. Thermal cycling conditions were denaturation at 95 °C for 10 min followed by 35 cycles at 95 °C for 15 s and 58 °C for 1 min. C- and N-terminal primers of target molecules were designed as follows: GAPDH forward, 5′-aaatggtgaaggtcggtgtg-3′, and reverse, 5′-tcgttgatgg caacaatctc-3′; and TMEM174 forward, 5′-taccctcaagacaatgctgc-3′, and reverse, 5′-tggaggagagaaacatacgca-3′.

2.9. Statistical analysis

Frequencies of nucleotide changes in normoglycemic controls and lean diabetes subjects were compared by the Pearson's chi-squared test or the Fisher's exact test, wherever appropriate.

2.10. Ethics

Ethical approval for this study was given by the Institutional Review Board and Ethics Committee of Kyoto University School of Medicine, Kyoto University, Japan (approval number: G267; approval date: 9 October 2008). Written, informed consent was obtained from each participant. This study was carried out in accordance with the Declaration of Helsinki as revised in 2000.

3. Results

3.1. Characteristics of family members

A family with a 3-generation history of diabetes was enrolled in this study (Fig. 1, Table 1). Thirteen members (6 men, 7 women) had previously been diagnosed with diabetes, 9 of them before the age of 40. Nine of the 13 family members with diabetes were lean (BMI<25); none of them were both obese and late-onset (later than 40). Eight family members were treated with oral antidiabetic drugs and 1 with insulin.

3.2. Detection of a diabetes susceptibility mutation in the hepatocyte nuclear factor 4 alpha (HNF4A) gene

For the index case, we performed direct sequencing in entire coding exons of the 6 MODY genes. The detected missense SNPs were the p.S487N variant of *HNF1A* (rs2464196) and the p.T130I variant of *HNF4A* (rs1800961) (Supplementary Table 3). The p.T130I variant of *HNF4A* was not a cause of MODY but was associated with late-onset type 2 diabetes in a previous report [13], so we genotyped all family members for the variant. As a result, 6 members with diabetes and 1 member without diabetes were found to be heterozygous for the variant (Fig. 1). We hypothesized that the disease susceptibility variant for the 6 members with diabetes was the p.T130I variant of *HNF4A*. We detected no copy number losses in *HNF1A*, *HNF1B*, and *GCK* on the index case (Supplementary Table 4).

3.3. Linkage analysis

We performed linkage analysis to identify the susceptibility gene in the family members with diabetes and also negative for the p.T130I variant of *HNF4A*. Family members positive for the variant were assigned as having unknown phenotype in the linkage analysis. A total of 12 family members (7 assigned as having affected phenotype, 4 assigned as having unknown phenotype, and 1 assigned as having unaffected phenotype) were included in the linkage analysis, assuming an autosomal dominant model. The genome-wide linkage results in the screening are shown in Fig. 2. Regions of potential interest by the multipoint LOD score were observed on chromosomes 4, 5 and 12. After fine mapping, 4q34, 5q11–q13, and 12p11–q22 were revealed to be candidate regions (Supplementary Table 5, LOD = 1.80).

3.4. Candidate variants in exome sequencing

We searched candidate genetic variants in the implicated linkage region by performing exome sequencing in family member II-2, who was negative for mutations in the exons of the 6 MODY genes. Family member II-2 was also negative for copy number losses in *HNF1A*, *HNF1B*, and *GCK* (Supplementary Table 4). The exome DNA library of the family member was sequenced in 76 bp paired-end reads, using 2 channels of Genome Analyzer IIx. We generated approximately 153 million reads and 98.02% of the reads were mapped to the reference human genome (Ghr37/hg19). On target rate to the bait was 59.1% and coverage depth was ≥3 in 97.40% of the targeted region and ≥20 in 87.11% of the targeted region. We predicted that the familial clustering of diabetes is caused by a rare non-synonymous variant, and focused our analysis on

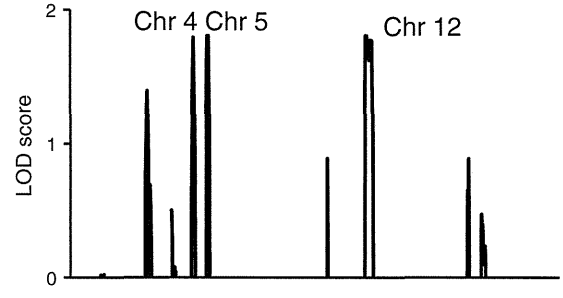

Fig. 2. Multipoint LOD scores in the genome-wide linkage analysis for the pedigree.

non-synonymous heterozygous or homozygous variants absent in the dbSNP131 (http://www.ncbi.nlm.nih.gov/projects/SNP/). In the implicated linkage region, we detected 10 such variants. All of these variants were heterozygous and were validated by Sanger method (Table 2). We genotyped all family members included in the linkage analysis for the 10 variants and 7 of them were detected in all affected family members without the p.T130I variant of *HNF4A*.

3.5. Allele frequencies of the candidate variants in cases and controls

To determine whether each of the 7 variants was rare or common in the general Japanese population without hyperglycemia, we genotyped 105 normoglycemic controls for the 7 variants. Minor allele frequencies ranged from 0.0% to 4.7% for the 7 variants (Table 3). We then genotyped 67 lean diabetes subjects to determine the frequency of the variants in a group predicted to be genetically predisposed to diabetes. The p.N1072K variant of *EEA1* was found to be significantly more frequent in the lean diabetes subjects than in the normoglycemic controls (0 in normoglycemic controls, 4 in lean diabetes subjects, $p = 0.022$, Fisher's exact test). Two of the 4 lean diabetes subjects had family history; the mother of one subject and a sibling of the other subject had diabetes, but DNA samples of their family members were unavailable. We also genotyped the p.N1072K variant of *EEA1* in another, unrelated 64 familial diabetes subjects and found 3 of them to be heterozygous for the variant; the minor allele frequency being 3/128 (2.3%). For 1 of the 3 subjects heterozygous for the variant, a DNA sample of a family member was available and the variant was concordant with the affection status in the family (Supplementary Fig. 1, Supplementary Table 6).

3.6. Linkage reanalysis of the family with a 3-generation history of diabetes

We performed a linkage analysis in the family with a 3-generation history of diabetes of chromosome 12 using the g.93175846 genotype in *EEA1* together with the microsatellite markers. We reassigned the affection status: subjects heterozygous for the p.N1072K variant of *EEA1* (II-1, II-2, II-4, II-5, II-6, II-7, III-1, III-2, and III-4) were considered as having affected phenotype and subjects negative for the variant (II-9 and III-3) were considered as having unaffected phenotype. We found a LOD score of 2.70 at the locus of the p.N1072K variant of *EEA1* (Fig. 3).

4. Discussion

In the present study, we analyzed a family with highly aggregated diabetes mellitus by combining exome sequencing and a linkage analysis. We identified a candidate susceptibility variant of *EEA1* in the linkage region located on chromosome 12p11–q22. The region has not been reported in previous linkage analyses with familial diabetes in Japan.

Table 2
Non-synonymous nucleotide changes in the linkage regions.

Gene	Chr:position (GRCh37) nucleotide change	Amino acid change	Concordance
SREK1IP1	5:64037004 G>A	R29C	+
CENPH	5:68490521 G>A	A80T	+
TMEM174	5:72469428 T>C	F120L	+
SMAGP	12:51640553 T>C	S33G	+
KRT78	12:53233268 C>T	M424I	−
NACA	12:57109861 G>A	P1818L	+
LRIG3	12:59274465 G>A	R567W	−
TMEM19	12:72092800 C>T	P253L	−
LRRIQ1	12:85449653 T>C	E361G	+
EEA1	12:93175846 A>T	N1072K	+

Table 3
Allele frequencies of candidate variants in the normoglycemic controls and the lean diabetes subjects.

Gene	Amino acid change	Detected number of alleles					
		Controls ($n=105$)			Diabetes ($n=67$)		
		Major	Minor	MAF	Major	Minor	MAF
SREK1IP1	R29C	200	10	0.047	126	8	0.059
CENPH	A80T	208	2	0.009	132	2	0.014
TMEM174	F120L	210	0	0.000	134	0	0.000
SMAGP	S33G	208	2	0.009	134	0	0.000
NACA	P1818L	204	6	0.029	134	0	0.000
LRRIQ1	E361G	209	1	0.004	132	2	0.014
EEA1	N1072K	210	0	0.000	130	4[a]	0.029

MAF = Minor Allele Frequency.
[a] Fisher's exact test, $p<0.05$.

The *EEA1* variant was detected in all affected family members without the p.T130I variant of *HNF4A*. We validated the candidate susceptibility variant of *EEA1* by performing a case–control study. The variant was significantly more frequent in the diabetes subjects than in the cohort of subjects that retained fasting normoglycemia for 5 years. It is important that the *EEA1* variant was not detected in 105 controls that are supposed to have protective genetic background against diabetes, because enough power to detect a polymorphism present in 1% of the control chromosomes was achieved by genotyping 105 individuals.

In several studies, exome sequencing has been performed to identify the cause of neonatal diabetes or familial diabetes and it has successfully identified the causal mutations in genes previously known to be involved in the pathogenesis of diabetes [14–17]. To our knowledge this is the first study to propose a new diabetes susceptibility gene by utilizing exome sequencing.

The EEA1 protein is known to localize exclusively to early endosomes. EEA1 is a membrane bound, endosome fusion promoting protein and an effector of the small GTPase Rab5 [18–20]. EEA1 is a coiled-coil homodimer with an N-terminal C_2H_2 zinc finger and a C-terminal region containing a calmodulin binding motif and a FYVE domain [21]. It is reported that EEA1 deficiency decreased insulin-stimulated glucose uptake and insulin-stimulated translocation of glucose transporter type 4 to the plasma membrane in human adipocytes [22]. Thus, the variant of *EEA1* could cause type 2 diabetes susceptibility by inducing insulin resistance. The Asn1024 residue of EEA1 is conserved among mammals [23], suggesting that a substitution to lysine might affect the function of EEA1; however, the residue is located on the coiled-coil domain not directly involved in the interaction with Rab5 GTPase or endosomal membrane [21]. Further study is necessary to evaluate the functional significance of the variant.

Our study has other limitations. First, the p.T130I variant of *HNF4A* is not a cause of MODY and is reported to be found in non-diabetic individuals [13], so the possibility remains that the genetic cause of diabetes for

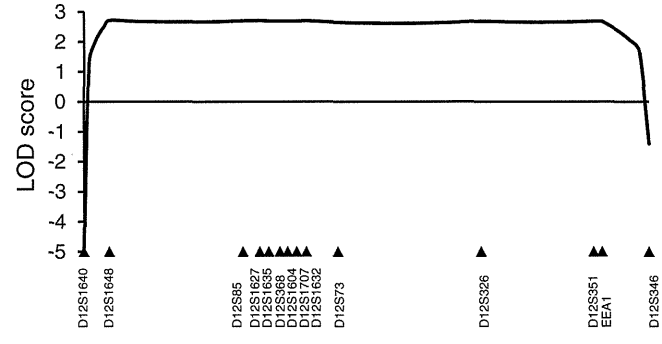

Fig. 3. Multipoint LOD scores for chromosome 12 after fine mapping and reassignment of the affection status.

members I-3, II-9, II-10, and III-3 in the family is not the p.T130I variant of *HNF4A*. Second, we focused only on nonsynonymous single nucleotide variants in the linkage region and eliminated a large number of insertion/deletions detected in the exome sequencing, most of which were not confirmed by the direct sequencing [24]. Third, in the linkage region, besides the p.N1072K variant of *EEA1*, p.F120L of *TMEM174* was also undetectable in the 105 control subjects and was considered rare. The p.F120L variant of *TMEM174* was not detected in the 67 diabetes subjects, but it might be an extremely rare diabetes susceptibility variant that is found specifically in this family. The PolyPhen-2 prediction score for the p.F120L variant of *TMEM174* was 0.990 and the variant was predicted to be probably damaging, and the p.T130I variant of *HNF4A* and the p.N1072K variant of *EEA1* were predicted to be benign with the prediction score of 0.001 and 0.191 respectively [25]. However, we thought that the TMEM174 gene is less likely to be the cause of diabetes than the EEA1 gene because the TMEM174 gene is almost specifically expressed in the kidney [26], not in the pancreatic islets or the liver according to our RT-PCR analysis using mouse tissues (Supplementary Fig. 2). Fourth, the LOD score at the locus of the p.N1072K variant of *EEA1* in the linkage analysis was slightly lower than the genome-wide significance level. This lower-than-expected LOD score may be attributable to the difficulties inherent to the genetic heterogeneity of diabetes.

5. Conclusion

We propose that the EEA1 gene is a candidate type 2 diabetes susceptibility gene. A family-based approach combined with exome sequencing may be a useful strategy to elucidate the complex genetic background of type 2 diabetes by identifying rare disease variants not detected by GWAS.

Supplementary data to this article can be found online at http://dx.doi.org/10.1016/j.ymgme.2013.02.010.

Acknowledgments

We thank K. Akitomo and S. Yasui for technical assistance. This work was supported by a grant for Research on Human Genome Tailor-Made from the Ministry of Health, Labor, and Welfare of Japan, a grant for Research on Drug Discovery Platform from the Ministry of Health, Labor, and Welfare of Japan, a grant for Intractable Disease Research Program from the Ministry of Health, Labor, and Welfare of Japan, Scientific Research Grants from the Ministry of Education, Culture, Sports, Science, and Technology of Japan, and a grant from Core Research for Evolutional Science and Technology (CREST) of Japan Science and Technology Cooperation, and by Kyoto University Global COE Program "Center for Frontier Medicine".

References

[1] International Diabetes Federation, IDF Diabetes Atlas, 5th ed., 2011.
[2] M. Imamura, S. Maeda, Genetics of type 2 diabetes: the GWAS era and future perspectives, Endocr. J. 58 (2011) 723–739, (Review).
[3] B.F. Voight, L.J. Scott, V. Steinthorsdottir, A.P. Morris, C. Dina, R.P. Welch, E. Zeggini, C. Huth, Y.S. Aulchenko, G. Thorleifsson, L.J. McCulloch, T. Ferreira, H. Grallert, N. Amin, G. Wu, C.J. Willer, S. Raychaudhuri, S.A. McCarroll, C. Langenberg, O.M. Hofmann, J. Dupuis, L. Qi, A.V. Segrè, M. van Hoek, P. Navarro, K. Ardlie, B. Balkau, R. Benediktsson, A.J. Bennett, R. Blagieva, E. Boerwinkle, L.L. Bonnycastle, K. Bengtsson Boström, B. Bravenboer, S. Bumpstead, N.P. Burtt, G. Charpentier, P.S. Chines, M. Cornelis, D.J. Couper, G. Crawford, A.S. Doney, K.S. Elliott, A.L. Elliott, M.R. Erdos, C.S. Fox, C.S. Franklin, M. Ganser, C. Gieger, N. Grarup, T. Green, S. Griffin, C.J. Groves, C. Guiducci, S. Hadjadj, N. Hassanali, C. Herder, B. Isomaa, A.U. Jackson, P.R. Johnson, T. Jørgensen, W.H. Kao, N. Klopp, A. Kong, P. Kraft, J. Kuusisto, T. Lauritzen, M. Li, A. Lieverse, C.M. Lindgren, V. Lyssenko, M. Marre, T. Meitinger, K. Midthjell, M.A. Morken, N. Narisu, P. Nilsson, K.R. Owen, F. Payne, J.R. Perry, A.K. Petersen, C. Platou, C. Proença, I. Prokopenko, W. Rathmann, N.W. Rayner, N.R. Robertson, G. Rocheleau, M. Roden, M.J. Sampson, R. Saxena, B.M. Shields, P. Shrader, G. Sigurdsson, T. Sparsø, K. Strassburger, H.M. Stringham, Q. Sun, A.J. Swift, B. Thorand, J. Tichet, T. Tuomi, R.M. van Dam, T.W. van Haeften, T. van Herpt, J.V. van Vliet-Ostaptchouk, G.B. Walters, M.N. Weedon, C. Wijmenga, J. Witteman, R.N. Bergman, S. Cauchi, F.S. Collins, A.L. Gloyn, U. Gyllensten, T. Hansen, W.A. Hide, G.A. Hitman, A. Hofman, D.J. Hunter, K. Hveem, M. Laakso, K.L. Mohlke, A.D. Morris, C.N. Palmer, P.P. Pramstaller, I. Rudan, E. Sijbrands, L.D. Stein, J. Tuomilehto, A. Uitterlinden, M. Walker, N.J. Wareham, R.M. Watanabe, G.R. Abecasis, B.O. Boehm, H. Campbell, M.J. Daly, A.T. Hattersley, F.B. Hu, J.B. Meigs, J.S. Pankow, O. Pedersen, H.E. Wichmann, I. Barroso, J.C. Florez, T.M. Frayling, L. Groop, R. Sladek, U. Thorsteinsdottir, J.F. Wilson, T. Illig, P. Froguel, C.M. van Duijn, K. Stefansson, D. Altshuler, M. Boehnke, M.I. McCarthy, M. investigators, G. Consortium, Twelve type 2 diabetes susceptibility loci identified through large-scale association analysis, Nat. Genet. 42 (2010) 579–589.
[4] K. Miyake, W. Yang, K. Hara, K. Yasuda, Y. Horikawa, H. Osawa, H. Furuta, M.C. Ng, Y. Hirota, H. Mori, K. Ido, K. Yamagata, Y. Hinokio, Y. Oka, N. Iwasaki, Y. Iwamoto, Y. Yamada, Y. Seino, H. Maegawa, A. Kashiwagi, H.Y. Wang, T. Tanahashi, N. Nakamura, J. Takeda, E. Maeda, K. Yamamoto, K. Tokunaga, R.C. Ma, W.Y. So, J.C. Chan, N. Kamatani, H. Makino, K. Nanjo, T. Kadowaki, M. Kasuga, Construction of a prediction model for type 2 diabetes mellitus in the Japanese population based on 11 genes with strong evidence of the association, J. Hum. Genet. 54 (2009) 236–241.
[5] W. Bodmer, C. Bonilla, Common and rare variants in multifactorial susceptibility to common diseases, Nat. Genet. 40 (2008) 695–701.
[6] W. Liu, D. Morito, S. Takashima, Y. Mineharu, H. Kobayashi, T. Hitomi, H. Hashikata, N. Matsuura, S. Yamazaki, A. Toyoda, K. Kikuta, Y. Takagi, K.H. Harada, A. Fujiyama, R. Herzig, B. Krischek, L. Zou, J.E. Kim, M. Kitakaze, S. Miyamoto, K. Nagata, N. Hashimoto, A. Koizumi, Identification of RNF213 as a susceptibility gene for moyamoya disease and its possible role in vascular development, PLoS One 6 (2011) e22542.
[7] K. Yamagata, Regulation of pancreatic beta-cell function by the HNF transcription network: lessons from maturity-onset diabetes of the young (MODY), Endocr. J. 50 (2003) 491–499.
[8] T. Yorifuji, R. Fujimaru, Y. Hosokawa, N. Tamagawa, M. Shiozaki, K. Aizu, K. Jinno, Y. Maruo, H. Nagasaka, T. Tajima, K. Kobayashi, T. Urakami, Comprehensive molecular analysis of Japanese patients with pediatric-onset MODY-type diabetes mellitus, Pediatr. Diabetes 13 (2012) 26–32.
[9] M.J. Bamshad, S.B. Ng, A.W. Bigham, H.K. Tabor, M.J. Emond, D.A. Nickerson, J. Shendure, Exome sequencing as a tool for Mendelian disease gene discovery, Nat. Rev. Genet. 12 (2011) 745–755.
[10] C.D. Saudek, W.H. Herman, D.B. Sacks, R.M. Bergenstal, D. Edelman, M.B. Davidson, A new look at screening and diagnosing diabetes mellitus, J. Clin. Endocrinol. Metab. 93 (2008) 2447–2453.
[11] S. Ellard, C. Bellanné-Chantelot, A.T. Hattersley, E.M.G.Q.N.E.M. group, Best practice guidelines for the molecular genetic diagnosis of maturity-onset diabetes of the young, Diabetologia 51 (2008) 546–553.
[12] L. Kruglyak, M.J. Daly, M.P. Reeve-Daly, E.S. Lander, Parametric and nonparametric linkage analysis: a unified multipoint approach, Am. J. Hum. Genet. 58 (1996) 1347–1363.
[13] Q. Zhu, K. Yamagata, A. Miura, N. Shihara, Y. Horikawa, J. Takeda, J. Miyagawa, Y. Matsuzawa, T130I mutation in HNF-4alpha gene is a loss-of-function mutation in hepatocytes and is associated with late-onset Type 2 diabetes mellitus in Japanese subjects, Diabetologia 46 (2003) 567–573.
[14] A. Bonnefond, E. Durand, O. Sand, F. De Graeve, S. Gallina, K. Busiah, S. Lobbens, A. Simon, C. Bellanné-Chantelot, L. Létourneau, R. Scharfmann, J. Delplanque, R. Sladek, M. Polak, M. Vaxillaire, P. Froguel, Molecular diagnosis of neonatal diabetes mellitus using next-generation sequencing of the whole exome, PLoS One 5 (2010) e13630.
[15] S. Johansson, H. Irgens, K.K. Chudasama, J. Molnes, J. Aerts, F.S. Roque, I. Jonassen, S. Levy, K. Lima, P.M. Knappskog, G.I. Bell, A. Molven, P.R. Njølstad, Exome sequencing and genetic testing for MODY, PLoS One 7 (2012) e38050.
[16] A. Bonnefond, J. Philippe, E. Durand, A. Dechaume, M. Huyvaert, L. Montagne, M. Marre, B. Balkau, I. Fajardy, A. Vambergue, V. Vatin, J. Delplanque, D. Le Guilcher, F. De Graeve, C. Lecoeur, O. Sand, M. Vaxillaire, P. Froguel, Whole-exome sequencing and high throughput genotyping identified KCNJ11 as the thirteenth MODY gene, PLoS One 7 (2012) e37423.
[17] D.S. Lieber, S.B. Vafai, L.C. Horton, N.G. Slate, S. Liu, M.L. Borowsky, S.E. Calvo, J.D. Schmahmann, V.K. Mootha, Atypical case of Wolfram syndrome revealed through targeted exome sequencing in a patient with suspected mitochondrial disease, BMC Med. Genet. 13 (2012) 3.
[18] F.T. Mu, J.M. Callaghan, O. Steele-Mortimer, H. Stenmark, R.G. Parton, P.L. Campbell, J. McCluskey, J.P. Yeo, E.P. Tock, B.H. Toh, EEA1, an early endosome-associated protein. EEA1 is a conserved alpha-helical peripheral membrane protein flanked by cysteine "fingers" and contains a calmodulin-binding IQ motif, J. Biol. Chem. 270 (1995) 13503–13511.
[19] H. Stenmark, R. Aasland, B.H. Toh, A. D'Arrigo, Endosomal localization of the autoantigen EEA1 is mediated by a zinc-binding FYVE finger, J. Biol. Chem. 271 (1996) 24048–24054.
[20] A. Simonsen, R. Lippé, S. Christoforidis, J.M. Gaullier, A. Brech, J. Callaghan, B.H. Toh, C. Murphy, M. Zerial, H. Stenmark, EEA1 links PI(3)K function to Rab5 regulation of endosome fusion, Nature 394 (1998) 494–498.
[21] J.J. Dumas, E. Merithew, E. Sudharshan, D. Rajamani, S. Hayes, D. Lawe, S. Corvera, D.G. Lambright, Multivalent endosome targeting by homodimeric EEA1, Mol. Cell 8 (2001) 947–958.
[22] R. Cheng, J. Qiu, X.Y. Zhou, X.H. Chen, C. Zhu, D.N. Qin, J.W. Wang, Y.H. Ni, C.B. Ji, X.R. Guo, Knockdown of STEAP4 inhibits insulin-stimulated glucose transport and GLUT4 translocation via attenuated phosphorylation of Akt, independent of the effects of EEA1, Mol. Med. Rep. 4 (2011) 519–523.
[23] P.A. Fujita, B. Rhead, A.S. Zweig, A.S. Hinrichs, D. Karolchik, M.S. Cline, M. Goldman, G.P. Barber, H. Clawson, A. Coelho, M. Diekhans, T.R. Dreszer, B.M. Giardine, R.A. Harte, J. Hillman-Jackson, F. Hsu, V. Kirkup, R.M. Kuhn, K. Learned,

C.H. Li, L.R. Meyer, A. Pohl, B.J. Raney, K.R. Rosenbloom, K.E. Smith, D. Haussler, W.J. Kent, The UCSC genome browser database: update 2011, Nucleic Acids Res. 39 (2011) D876–D882.

[24] E. Karakoc, C. Alkan, B.J. O'Roak, M.Y. Dennis, L. Vives, K. Mark, M.J. Rieder, D.A. Nickerson, E.E. Eichler, Detection of structural variants and indels within exome data, Nat. Methods 9 (2012) 176–178.

[25] I.A. Adzhubei, S. Schmidt, L. Peshkin, V.E. Ramensky, A. Gerasimova, P. Bork, A.S. Kondrashov, S.R. Sunyaev, A method and server for predicting damaging missense mutations, Nat. Methods 7 (2010) 248–249.

[26] P. Wang, B. Sun, D. Hao, X. Zhang, T. Shi, D. Ma, Human TMEM174 that is highly expressed in kidney tissue activates AP-1 and promotes cell proliferation, Biochem. Biophys. Res. Commun. 394 (2010) 993–999.

Clinical and functional characterization of the Pro1198Leu *ABCC8* gene mutation associated with permanent neonatal diabetes mellitus

Tomoyuki Takagi[1], Hiroto Furuta[1]*, Masakazu Miyawaki[2], Kazuaki Nagashima[3], Takeshi Shimada[1], Asako Doi[1], Shohei Matsuno[1], Daisuke Tanaka[3], Masahiro Nishi[1], Hideyuki Sasaki[1], Nobuya Inagaki[3], Norishige Yoshikawa[2], Kishio Nanjo[4], Takashi Akamizu[1]

ABSTRACT

Aims/Introduction: The adenosine triphosphate (ATP)-sensitive potassium (K_{ATP}) channel is a key component of insulin secretion in pancreatic β-cells. Activating mutations in *ABCC8* encoding for the sulfonylurea receptor subunit of the K_{ATP} channel have been associated with the development of neonatal diabetes mellitus (NDM). The aim was to investigate clinical and functional characterization of the Pro1198Leu *ABCC8* gene mutation associated with permanent NDM (PNDM).

Materials and Methods: The coding regions and conserved splice sites of *KCNJ11*, *ABCC8* and *INS* were screened for mutations in a 12-year-old girl diagnosed with PNDM. The functional property of the mutant channel identified was examined with patch-clamp experiments in COS-1 cells. We also investigated the difference of effectiveness between two groups of oral sulfonylureas *in vitro* and in the patient.

Results: We identified a heterozygous missense mutation (c.3593 C>T, Pro1198Leu) in *ABCC8*. The mutated residue (P1198) is located within a putative binding site of sulfonylureas, such as tolbutamide or gliclazide. In patch-clamp experiments, the mutant channel was less ATP sensitive than the wild type. Furthermore, the sensitivity to tolbutamide was also reduced in the mutant channel. In addition to the tolbutamide/gliclazide binding site, glibenclamide is thought to also bind to another site. Glibenclamide was more effective than other sulfonylureas *in vitro* and in the patient. The treatment of the patient was finally able to be switched from insulin injection to oral glibenclamide.

Conclusions: We identified the Pro1198Leu *ABCC8* mutation in a PNDM patient, and clarified the functional and clinical characterization. The present findings provide new information for understanding PNDM. (J Diabetes Invest, doi: 10.1111/jdi.12049, 2013)

KEY WORDS: *ABCC8*, Neonatal diabetes, Sulfonylurea receptor

INTRODUCTION

Neonatal diabetes mellitus (NDM) is a specific form of diabetes[1]. It has been defined as diabetes with onset before 6 months-of-age and autoantibody negative for type 1 diabetes in general. NDM is classified into two categories clinically. One is transient NDM (TNDM), in which diabetes develops within the first few weeks of life and resolves by a few months of age, although it might frequently relapse in adolescence or young adulthood. The other is permanent NDM (PNDM), in which diabetes does not remit and the patients usually require insulin treatment for life. Approximately 50% of NDM is transient and 50% is permanent[2]. The majority (~70%) of cases of TNDM have abnormalities in the imprinted region of chromosome 6q24, such as paternal uniparental isodisomy, paternally inherited duplication and maternal methylation defects, leading to overexpression of paternally expressed genes[3]. The adenosine triphosphate (ATP)-sensitive potassium (K_{ATP}) channel is a key component of insulin secretion in pancreatic β-cells. The channel is comprised of two proteins, an inwardly rectifying potassium ion pore-forming subunit (Kir6.2; encoded by *KCNJ11*) and a high-affinity β-cell sulfonylurea receptor (SUR1; encoded by *ABCC8*)[4]. Activating mutations in *KCNJ11* and *ABCC8* account for 12% and 13% of cases of TNDM, respectively[5]. They also account for 31% and 10% of cases of PNDM, respectively[6]. Furthermore, 12% of PNDM is caused by mutations in the insulin (*INS*) gene itself[6]. It has also been reported that a few cases of PNDM are attributed to genetic abnormalities in other genes, such as *GCK*, *FOXP3*, *EIF2AK3*, *PDX1*, *PTF1A*, *GLIS3*, *NEUROD1* and *HNF1B*, which are important to pancreatic β-cell function and development[1].

The K_{ATP} channel plays a key role in glucose-dependent insulin secretion from pancreatic β-cells. After entry of glucose into

[1]First Department of Medicine and [2]Department of Pediatrics, Wakayama Medical University, [4]Wakayama Rosai Hospital, Wakayama, and [3]Department of Diabetes and Clinical Nutrition, Graduate School of Medicine, Kyoto University, Kyoto, Japan
*Corresponding author. Hiroto Furuta Tel.: +81-73-441-0625 Fax: +81-73-445-9436
E-mail address: hfuruta@wakayama-med.ac.jp
Received 29 October 2012; revised 15 November 2012; accepted 20 November 2012

the β-cells, glucose is metabolized and ATP is produced. The elevated intracellular ATP levels cause closure of K_{ATP} channels on the cell surface, which then depolarize the cell membrane leading to opening of the voltage-dependent calcium channels. The resultant influx of calcium triggers a cascade of events that result in the secretion of insulin. Overactive mutant channels as a result of activating mutations in *KCNJ11* or *ABCC8*, therefore, hyperpolarize the cell membrane, reduce calcium influx and decrease insulin secretion. Sulfonylureas bind to the SUR1 subunit of the K_{ATP} channel, and close the channel in an ATP-independent manner. It has been reported that oral sulfonylurea administration increases insulin secretion and improves metabolic control in patients with PNDM as a result of activating mutations in *KCNJ11* and *ABCC8*[7,8]. In the present study, we investigated genetic abnormalities in a patient with PNDM, and found the Pro1198Leu mutation in *ABCC8*. We examined the functional property of a mutant channel with the patch-clamp experiments, and the clinical response to oral sulfonylurea administration.

MATERIALS AND METHODS

Mutation Screening

The proband is a 12-year-old girl. She was born after 38 weeks of an uneventful pregnancy with a birthweight of 2778 g (just under the 50th percentile). At 28 weeks-of-age, she presented with severe hyperglycemia (blood glucose 915 mg/dL, glycated hemoglobin [HbA_{1c}] 12.8%) with ketoacidosis. The HbA_{1c} value was estimated as a National Glycohemoglobin Standardization Program (NGSP) equivalent value calculated by the formula HbA_{1c} = HbA_{1c} (Japan Diabetes Society [JDS]) + 0.5%, considering the relational expression of HbA_{1c} (JDS) measured by the previous Japanese standard substance and measurement methods, and HbA_{1c} (NGSP)[9]. Fasting serum C-peptide level was undetectable (<0.5 ng/mL) at first, but it was recovered to 0.9 ng/mL after 2 months of treatment with insulin. NDM is defined as diabetes with onset before 6 months-of-age in general. As her HbA_{1c} at the time of diagnosis was notably high, it could be speculated that her plasma glucose had been elevated before 6 months-of-age. Her medical record of bodyweight also suggested that failure to thrive had started from 5 months-of-age. No neurological abnormality was observed, and anti-glutamic acid decarboxylase (GAD) antibody was undetectable. Abdominal ultrasound examination at the age of 12 years showed a normally-developed pancreas. She had been treated with insulin from the onset of diabetes. The pedigree of the family is shown in Figure 1.

After obtaining written informed consent, genomic DNA was isolated from peripheral blood leukocytes. The coding regions and conserved splice sites of *KCNJ11, ABCC8* and *INS* were amplified from genomic DNA by polymerase chain reaction using specific primers (Supporting Information Table S1). The products were sequenced using Dye Terminator chemistry on an ABI 3100 (Applied Biosystems, Warrington, UK). The study protocol was approved by the institutional review board.

Functional Analysis of Mutant K_{ATP} Channel

The mammalian expression plasmids containing the whole coding region of the human Kir6.2 and SUR1 have been described previously[4,10]. We generated the expression plasmid of SUR1

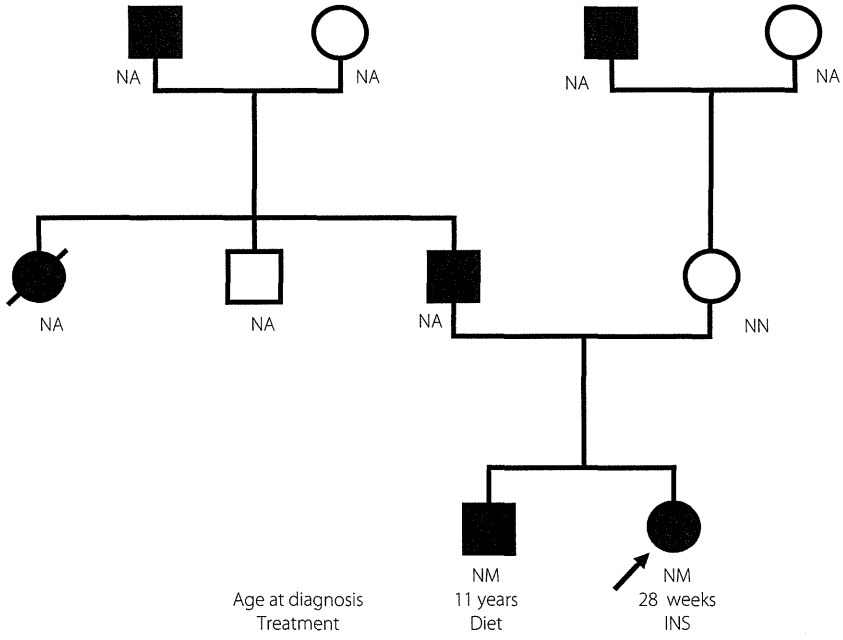

Figure 1 | Pedigree of the family. The allele status is indicated under the symbols. Directly below the genotype is the age of diagnosis of diabetes and treatment. INS, insulin; NA, not available for testing; NM, one normal and one mutated allele; NN, two normal alleles; OHA, oral hypoglycemic agent.